Bio-based succinate from sucrose: High-resolution 13 C metabolic flux analysis and metabolic engineering of the rumen bacterium Basfia succiniciproducens

Anna Lange, Judith Becker, Dennis Schulze, Edern Cahoreau, Jean-Charles Portais, Stefan Haefner, Hartwig Schröder, Joanna Krawczyk, Oskar Zelder, Christoph Wittmann

Metabolic Engineering 44 (2017) 198–212

Contents lists available at ScienceDirect

Metabolic Engineering

journal homepage: www.elsevier.com/locate/meteng

Bio-based succinate from sucrose: High-resolution ^{13}C metabolic flux analysis and metabolic engineering of the rumen bacterium *Basfia succiniciproducens*

Anna Lange[a], Judith Becker[a], Dennis Schulze[a], Edern Cahoreau[b,c,d], Jean-Charles Portais[b,c,d], Stefan Haefner[e], Hartwig Schröder[e], Joanna Krawczyk[e], Oskar Zelder[e], Christoph Wittmann[a,*]

[a] *Institute of Systems Biotechnology, Saarland University, Germany*
[b] *Université de Toulouse, INSA, UPS, INP, Toulouse, France*
[c] *INRA, UMR792 Ingénierie des Systèmes Biologiques et des Procédés, Toulouse, France*
[d] *CNRS, UMR5504, Toulouse, France*
[e] *BASF SE, Fine Chemicals and Biotechnology, Ludwigshafen, Germany*

ARTICLE INFO

Keywords:
^{13}C metabolic flux analysis
Mass spectrometry
Isotopomer
OpenFLUX
Succinate, succinic acid
Sucrose
Metabolic engineering
Fructose phosphotransferase system
Fructokinase
Fructose

ABSTRACT

Succinic acid is a platform chemical of recognized industrial value and accordingly faces a continuous challenge to enable manufacturing from most attractive raw materials. It is mainly produced from glucose, using microbial fermentation. Here, we explore and optimize succinate production from sucrose, a globally applied substrate in biotechnology, using the rumen bacterium *Basfia succiniciproducens* DD1. As basis of the strain optimization, the yet unknown sucrose metabolism of the microbe was studied, using ^{13}C metabolic flux analyses. When grown in batch culture on sucrose, the bacterium exhibited a high succinate yield of 1 mol mol^{-1} and a by-product spectrum, which did not match the expected PTS-mediated sucrose catabolism. This led to the discovery of a fructokinase, involved in sucrose catabolism. The flux approach unraveled that the fructokinase and the fructose PTS both contribute to phosphorylation of the fructose part of sucrose. The contribution of the fructokinase reduces the undesired loss of the succinate precursor PEP into pyruvate and into pyruvate-derived by-products and enables increased succinate production, exclusively via the reductive TCA cycle branch. These findings were used to design superior producers. Mutants, which (i) overexpress the beneficial fructokinase, (II) lack the competing fructose PTS, and (iii) combine both traits, produce significantly more succinate. In a fed-batch process, *B. succiniciproducens* Δ*fruA* achieved a titer of 71 g L^{-1} succinate and a yield of 2.5 mol mol^{-1} from sucrose.

1. Introduction

Bio-based succinate has received considerable attention, owing to its huge potential as a sustainable platform chemical (Becker et al., 2015); it is produced at an industrial scale (Ahn et al., 2016). Companies such as BioAmber, Myriant, Reverdia, and Succinity have announced the production of several thousand tons of succinate per year. In recent years, a broad array of microorganisms, including bacteria and yeasts, has been evaluated for their succinate production capacity and performance, mainly from glucose and starchy materials (Ahn et al., 2016).

One of the most promising producers is the facultative anaerobic and capnophilic rumen bacterium *Basfia succiniciproducens*, which belongs to the family of *Pasteurellaceae* (Kuhnert et al., 2010). When grown in the absence of oxygen, it uses fumarate as the final electron acceptor and secretes succinate, while efficiently fixing CO_2. The wild type *B. succiniciproducens* DD1 achieves succinate yields of up to 75%, making it an attractive bacterium for the production of commercial quantities of bio-based succinate for the global market (Becker et al., 2013). *B. succiniciproducens* does not harbor any amino acid auxotrophy despite its rather small genome size, which facilitates the use of cheap and lean production media.

The microbe exhibits a broad substrate spectrum and utilizes a range of sugars and sugar alcohols, e.g. glucose, galactose, mannose, sucrose, trehalose and xylose, mannitol, and glycerol (Kuhnert et al., 2010; Scholten and Dägele, 2008). With regard to regional availability and fluctuating raw material costs, however, there is evidently a need to extend research and development to other carbon sources. Therefore,

* Correspondence to: Saarland University, Campus A1.5, 66123 Saarbrücken, Germany.
E-mail address: christoph.wittmann@uni-saarland.de (C. Wittmann).

http://dx.doi.org/10.1016/j.ymben.2017.10.003
Received 30 May 2017; Received in revised form 10 September 2017; Accepted 4 October 2017
Available online 14 October 2017

Table 1
Basfia succiniciproducens strains used in the present work.

Strain	Description	Reference
DD1	Wild type isolate of *B. succiniciproducens*	Kuhnert et al. (2010)
Δ*pflD*	DD1 + deletion of the *pflD* gene, encoding pyruvate-formate lyase	Becker et al. (2013)
Δ*ldhA*	DD1 + deletion of the *ldhA* gene, encoding D-lactate dehydrogenase	This work
Δ*fruA*	DD1 + deletion of the *fruA* gene, encoding fructose PTS	This work
DD1*	DD1, carrying the empty, episomally replicating vector pJFF224	This work
Δ*fruA**	Δ*fruA*, carrying the empty, episomally replicating vector pJFF224	This work
DD1 P_{ackA}*rbsK*	DD1 + pJFF244-mediated episomal expression of the *rbsK* gene, encoding fructokinase, under the control of the promoter of *ackA*, encoding acetate kinase.	This work
Δ*fruA* P_{ackA}*rbsK*	Δ*fruA* + pJFF2440-mediated episomal expression of the *rbsK* gene, encoding fructokinase, under the control of the promoter of *ackA*, encoding acetate kinase.	This work

research has intensively focused on the utilization of different substrates for producing succinate, involving amongst others, glucose (Becker et al., 2013), sucrose (Schröder et al., 2014), glycerol (Scholten et al., 2009), lignocellulosic hydrolysates (Salvachua et al., 2016), and mixtures of maltose and glycerol (Schröder et al., 2014). A particularly interesting substrate is sucrose, a disaccharide composed of glucose and fructose. Sucrose is the feedstock for more than half of the world's fuel ethanol production and harvested primarily from sugarcane and beet (Wu and Birch, 2007). In addition to its use as raw sugar, sucrose is frequently used for bio-production in the form of molasses - a waste product of sugar refinement (Liu et al., 2008). As demonstrated, *B. succiniciproducens* produces sucicnate from sucrose (Kuhnert et al., 2010).

Enzymatic and gene knockout studies in *Mannheimia succiniciproducens* (*Pasteurellaceae*) indicate that rumen bacteria orchestrate a set of enzymes to utilize sucrose: (i) a sucrose phosphotransferase system (PTS) for sucrose uptake (*ptsG*), (ii) a sucrose 6-phosphate hydrolase (*sacC*), which forms glucose 6-phosphate and fructose, (iii) a fructose PTS (*fruA*), which phosphorylates the fructose subunit into fructose 1-phosphate, and (v) a phosphofructokinase, which then forms fructose 1,6-bisphosphate, an intermediate of the glycolytic chain (Lee et al., 2010). A peculiarity in rumen bacteria is the genomic organization of their sucrose utilization genes. Unlike that in other microorganisms, they are not located in a single cluster under control of a sucrose-specific repressor, allowing for simultaneous consumption of sucrose, glucose, and fructose (Lee et al., 2010).

In this work, the production of succinate from sucrose in *B. succiniproducens* was studied and optimized. Based on the success of previous studies (Arifin et al., 2014; Wittmann et al., 2004), ^{13}C metabolic flux analysis was conducted, to explore the practically unstudied sucrose metabolism in the microbe on a quantitative level. To this end, a comprehensive experimental and computational approach was established. To account for the complexity of the substrate, composed of two different sugars, four parallel ^{13}C tracer experiments with different substrate labeling were designed and conducted, followed by GC/MS analysis of 460 individual mass isotopomers of intracellular and secreted metabolites. The obtained data provide a fascinating insight into growth and succinate production from sucrose. A newly discovered fructokinase and the fructose PTS were identified as genetic targets for systems metabolic engineering of *B. succiniciproducens*. The predicted mutants were constructed and evaluated.

2. Materials and methods

2.1. Strains, plasmids, and genetic engineering

Wild type *B. succiniciproducens* DD1 (Kuhnert et al., 2010) and the deletion strain *B. succiniciproducens* DD1 Δ*pflD* (Becker et al., 2013) were obtained from previous work. *Escherichia coli* TOP10 (Invitrogen, Darmstadt, Germany) was used as the host for vector amplification. For maintenance, cells were kept as glycerol stocks at −80 °C. Vector and strain construction were conducted using standard techniques as described previously (Becker et al., 2013). Specific primer sequences used for strain construction and validation are given in Table S1. Marker free deletion of *ldhA* was performed as described previously (Becker et al., 2013). Marker free deletion of *fruA*, encoding the fructose PTS, used the integrative vector pClik^{CM} (Becker et al., 2011) and the primers $PR_{fruA}1$–$PR_{fruA}4$ (Table S1). The *fruA* deletion fragment was ligated into the vector pClik^{CM} via the restriction sites *Xba*I and *Xho*I. Desired elimination of *fruA* in the genome was verified by PCR. For overexpression of fructokinase (*rbsK)*, the episomal plasmid pJFF224 (Frey, 1992) was used. The gene was expressed under control of the promoter *ackA*, encoding acetate kinase. For seamless fusion of promoter and gene, overlap extension PCR was applied. To this end, the *ackA* promoter and the *rbsK* gene were first amplified using the primer combinations $PR_{rbsK}1$/$PR_{rbsK}2$ and $PR_{rbsK}3$/$PR_{rbsK}4$, respectively. The resulting PCR fragments were then fused to the 1520 bp promoter gene construct using $PR_{rbsK}1$/$PR_{rbsK}4$. Subcloning of the P_{ackA}*rbsK* construct into the *XbaI*- and *XhoI*-digested vector pJFF224, using the InFusion kit (Clontech Laboratories, Mountain View, CA, Usuccinate), yielded the plasmid pJFF224_P_{ackA}*rbsK*. Transformation of *B. succiniciproducens* with pJFF224 and pJFF224_P_{ackA}*rbsK* was carried out by electroporation (Becker et al., 2011). The resulting mutants (Table 1) were analyzed by PCR and enzyme activity studies. PCR was routinely performed with proof-reading polymerases (Phusion High-Fidelity PCR Kit, Thermo Fisher Scientific, Schwerte, Germany).

2.2. Media

For physiological studies, the first pre-cultivation of *B. succiniciproducens* was conducted in complex medium, which contained per liter: 50 g sucrose, 5 g yeast extract (Becton Dickinson, Franklin Lakes, NJ, US), 5 g bacto peptone (Becton Dickinson), 1 g NaCl, 0.2 g $MgCl_2{\cdot}6H_2O$, 0.2 g $CaCl_2{\cdot}2H_2O$, 3 g K_2HPO_4, 1 g $(NH_4)_2SO_4$, and 50 g $MgCO_3$. For the second pre-cultivation and subsequent main cultivation, a minimal medium was used, which contained per liter: 50 g sucrose, 1 g NaCl, 0.2 g $MgCl_2{\cdot}6H_2O$, 0.2 g $CaCl_2{\cdot}2H_2O$, 3 g K_2HPO_4, 5 g $(NH_4)_2SO_4$, 3 mg thiamin·HCl, 0.6 mg riboflavin, 3 mg nicotinic acid, 10 mg Ca-pantothenate, 1 mg pyridoxal·HCl, 0.5 mg biotin, 0.05 mg cyanocobalamin, and 50 g $MgCO_3$. Carbon dioxide was applied to the culture bottles at 0.8 bar overpressure. For cultivation of plasmid-containing strains, chloramphenicol was added to a final concentration of 50 μg mL^{-1}. For isotopic tracer studies, naturally labeled substrates were replaced by equimolar amounts of ^{13}C-labeled substrates. To resolve the fluxes of interest, four different tracer substrates were used in parallel experiments. Instead of naturally labeled sucrose, three set-ups contained (i) 99% [1-$^{13}C^{Frc}$] sucrose, (ii) 99% [1-$^{13}C^{Glc}$] sucrose, or (iii) 99% [$^{13}C_6^{Frc}$] sucrose (Omicron Biochemicals, South Bend, Indiana, US). In a fourth set-up, naturally labeled $MgCO_3$ was replaced by 98% $Mg^{13}CO_3$ (Sigma Aldrich, Taufkirchen, Germany), and 99% $^{13}CO_2$ (Sigma Aldrich) was used at 0.8 bar overpressure, instead of naturally labeled CO_2. In additional studies, the medium was supplemented with

[$^{13}C_2$] acetate (Sigma Aldrich), as specified below. For enzyme assays, cells were grown in minimal medium containing the same components as previously mentioned, except the $MgCO_3$, with automated addition of 1 M Na_2CO_3 for pH control. For fed-batch production, the pre-culture was grown on complex medium containing 50 g sucrose, 5 g yeast extract (Becton Dickinson), 5 g bacto peptone (Becton Dickinson), 1 g NaCl, 0.2 g $MgCl_2{\cdot}6H_2O$, 0.2 g $CaCl_2{\cdot}2H_2O$, 3 g K_2HPO_4, 1 g $(NH_4)_2SO_4$, in addition to 3 mg thiamin·HCl, 0.6 mg riboflavin, 3 mg nicotinic acid, 10 mg Ca-pantothenate, 1 mg pyridoxal·HCl, 0.5 mg biotin, 0.05 mg cyanocobalamin, and 50 g $MgCO_3$. The medium for the initial batch phase in the bioreactor contained per liter: 25 g sucrose, 3.5 $(NH_4)_2SO_4$, 1.5 g K_2HPO_4, 3.5 g $(NH_4)_2HPO_4$, 1.5 mg $FeSO_4{\cdot}7H_2O$, 0.2 mg $MnCl_2{\cdot}4H_2O$, 0.4 mg $ZnSO_4{\cdot}7H_2O$, 7.5 µg $Na_2MoO_4{\cdot}6H_2O$, 20 µg $CoCl_2{\cdot}4H_2O$, 6.4 µg $NiCl_2{\cdot}6H_2O$, 2 µg Na_2SeO_3, 2.7 g citric acid, 1 mg thiamin·HCl, 1 mg riboflavin, 1 mg nicotinic acid, 1 mg Ca-pantothenate, 1 mg pyridoxal·HCl, 0.5 mg biotin, and 0.05 mg cyanocobalamin. The feed solution contained 800 g sucrose per liter. For genetic engineering and strain maintenance, complex medium, containing 37 g L^{-1} BHI (Becton Dickinson) was used. If required, 18 g L^{-1} agar (Becton Dickinson) was added to obtain solid medium.

2.3. Anaerobic cultivation in serum flasks

Cultivations were conducted in 30 mL serum bottles, equipped with butyl rubber seals for sampling, and filled with 10 mL medium under a CO_2 atmosphere at 0.8 bar overpressure. After inoculation from cryostocks, the first pre-culture was incubated for 8 h at 37 °C and placed on an orbital shaker (130 rpm). During exponential growth, cells were harvested by centrifugation (3 min, 16,000 *xg*, 16 °C), washed with 1 mL medium, and used to inoculate the second pre-culture to an initial optical density (OD_{600}) of 0.3. After 10 h of incubation, exponentially growing cells were harvested and washed as described above, and were then used to inoculate the main culture to an initial OD_{600} of 0.08. This low-OD_{600} inoculum prevented the potential interference of ^{13}C labeling data—taken later as the basis for the flux calculation—with non-labeled metabolites from the pre-culture (Wittmann, 2007). All cultures were conducted at least as three biological replicates.

2.4. Fed-batch production of succinate

Fed-batch fermentation was carried out in 1 L Multifors bioreactors with Rushton impellers (Infors, Basel, Switzerland) filled with 600 mL batch medium. The CO_2 sparging rate was set to 60 mL min^{-1} and the stirrer speed was set to 300 min^{-1}. Process control and data monitoring was conducted by the process control software BaseLab (BASF, Ludwigshafen, Germany). The culture was inoculated with 60 mL cells, pre-grown for 6 h at 37 °C and 230 rpm on a rotary shaker on complex pre-culture medium. Throughout the process, the pH was maintained at 6.5 ± 0.2 by automatic addition of base solution (25% $Mg(OH)_2$, 7% NH_3). The temperature was maintained at 37 ± 0.05 °C. At the end of the batch phase, feeding at a constant feed rate of 2.42 g h^{-1} was initiated manually.

2.5. Quantification of cell and biomass concentration

The cell concentration (OD_{600}) was recorded as the optical density at 600 nm. Prior to the measurement, samples were diluted at least tenfold with 1 M HCl to completely dissolve $MgCO_3$ particles. Biomass concentration was derived from immediate optical density measurement by a correlation factor of 0.331 (g L^{-1}) $OD_{600}{}^{-1}$ (Becker et al., 2013).

2.6. Quantification and identification of substrates and products

Sucrose, fructose, and glucose were quantified in tenfold diluted culture supernatant, using HPLC (VWR Hitachi Chromaster, Tokyo, Japan) equipped with a desalting column (Micro-Guard Deashing Cartridge, 30 × 4.6 mm, Bio-Rad, Hercules, CA, Usuccinate), a guard column (MetaCarb 87 C Guard Column, 50 × 4.6 mm, Agilent Technologies), and a reversed-phase column (MetaCarb 87 C, 300 × 7.8 mm, Agilent Technologies, Santa Clara, CA, Usuccinate), using water as the mobile phase at 85 °C and 0.6 mL min^{-1}, and detection by refraction index measurement. Succinic acid, acetic acid, lactic acid, formic acid, fumaric acid, ethanol (Becker et al., 2013), and amino acids (Krömer et al., 2005) were analyzed using HPLC. Acetoin and 2-oxoisovaleric acid were quantified using ^1H NMR. Samples were subjected to analysis after centrifugation and filtration. A volume of 500 µL supernatant was mixed with 100 µL D_2O, containing trimethyl-silyl-propionic acid (d4) as the internal standard for spectra calibration and absolute quantification of compounds. NMR spectra were collected on an Avance II 500 MHz spectrometer (Bruker Corporation, Billerica, Massachusetts, US), equipped with a 5-mm z-gradient BBI probe, and on an Avance III 800 MHz spectrometer (Bruker), equipped with a 1.7-mm z-gradient QTCI cryoprobe. Data were collected and processed using the software TopSpin 3.0 (Bruker). The compounds were identified based on their ^1H-1D and 2D spectra (^1H–^1H TOCSY, ^1H–^{13}C HSQC, and ^1H–^{13}C HMBC), and identification was confirmed by comparison to the pure standards. All acquisitions were performed at 286 K and presaturation was used to suppress water signals for each NMR acquisition. Hereby, ^1H-1D spectra were acquired with a 30 ° pulse. The relaxation delay between scans was set to 10 s to ensure full signal recovery for optimal accuracy of quantitative measurements. Absolute quantification was performed on ^1H-1D spectra using TopSpin 3.0 (Bruker) and the 1D fitting software Chenomx 8.1 (Chenomx, Edmonton, Alberta, Canada). The biomass constituents were taken from previous work (Becker et al., 2013) and used to provide the anabolic precursor demand for biomass formation (Table S2).

2.7. Quantification of enzyme activity

For the preparation of crude cell-free extracts, cells were harvested by centrifugation (5 min, 5000 *xg*, 4 °C), washed with 100 mM Tris·HCl (0.75 mM dithiothreitol, pH 7.8), resuspended in the same buffer to a concentration of 0.33 (g cell wet weight) mL^{-1}, and then disrupted using a bench-top homogenizer (Precellys 24, Peqlab, VWR International GmbH, Darmstadt, Germany). Enzyme activities were quantified spectrophotometrically (Spectronic Helios, Thermo Electron Corporation, Waltham, Massachusetts, USA) at 37 °C. The assay conditions were taken from previous studies including specific modifications, where appropriate. Fructokinase (Helanto et al., 2006) was assayed in 100 mM Tris·HCl (pH 7.8, 10 mM $MgCl_2$), 1 U mL^{-1} glucose 6-phosphate dehydrogenase, 2 U mL^{-1} phosphoglucoisomerase, 1 mM $NADP^+$, and different concentrations of ATP (0–5 mM) and fructose (0–25 mM) to determine the kinetic parameters. Lactate dehydrogenase (Bunch et al., 1997) was assayed in 100 mM Tris·HCl (pH 7.8), containing 0.25 mM NADH and 25 mM sodium pyruvate. The activity measurement of malic enzyme was based on a previous protocol (Gourdon et al., 2000), whereby the buffer was adapted to 100 mM Tris·HCl (pH 7.8), containing 2 mM $MgCl_2$, 1 mM $NADP^+$, and 40 mM sodium L-malate. PEP carboxylase (Jetten and Sinskey, 1993) was assayed in 80 mM MOPS, 10 mM $MnCl_2$, 2 mM glutathione, 0.5 mM NADH, 10 U mL^{-1} malate dehydrogenase, and 10 mM PEP. PEP carboxykinase was assayed using the same mixture (Jetten and Sinskey, 1993), except that 30 mM aspartate and 2.5 mM ATP was added. The protocols for pyruvate kinase (Netzer et al., 2004) and isocitrate dehydrogenase (Becker et al., 2009) were used without further adaptation. The reactions were monitored via the change of absorbance at 340 nm. The protein content of cell extracts was determined using a BCA protein assay kit (Thermo Scientific, Rockford, IL, Usuccinate). Kinetic enzyme parameters were obtained by fitting the experimental data to the Michaelis-Menten type kinetic equation (OriginLab, Northhampton, MA, USA).

2.8. Mass isotopomer analysis by GC/MS and processing of ^{13}C labeling data

For the analysis of proteinogenic amino acids, cells (1 mg cell dry mass) were obtained by centrifugation (5 min, 16,000 *xg*, 4 °C), washed with 1 M HCl to dissolve the entire $MgCO_3$, and hydrolyzed by incubation in 6 M HCl [100 µL (mg cell dry mass^{-1})] for 24 h at 105 °C (Kiefer et al., 2004). Cell debris was removed by filtration (0.2 µm, Merck Millipore, Darmstadt, Germany). Subsequently, 15 µL of the hydrolysate was dried under a nitrogen flow. Derivatization and GC/MS-based analyses of the obtained proteinogenic amino acids were carried out as described previously (Kiefer et al., 2004; Wittmann et al., 2002). The labeling pattern of secreted succinic acid in the culture supernatant was analyzed as a t-butyl-dimethylsilyl derivate via the [M-57] fragment at *m/z* 289–294, as described previously (Becker et al., 2013). For ^{13}C analysis of the glucose monomer of glycogen, the sugar was first obtained by enzymatic digestion. Cells (1 mg cell dry mass) were collected by centrifugation (5 min, 16,000 *xg*, 4 °C), washed with 1 M HCl, and again with 20 mM Tris·HCl (pH 7.0). The obtained pellet was resuspended in 500 µL enzyme solution [70 U mL^{-1} amyloglucosidase (Sigma-Aldrich, St. Louis, Missouri, USA) and 1.2 kU mL^{-1} lysozyme (Sigma-Aldrich) in 20 mM Tris·HCl, pH 7.0] and incubated in a heating block at 37 °C for 3 h at 400 rpm. Subsequently, cell debris was removed by centrifugation (5 min, 16,000 *xg*, 4 °C) and subsequent filtration (0.2 µm, Merck Millipore). Glucose, derived from the enzymatic hydrolysis, was quantified enzymatically (Becker et al., 2009). An aliquot of 25 µg glucose was then dried by lyophilization, followed by incubation with 50 µL methoxylamine (2% in pyridine) for 25 min at 80 °C. Subsequently, 50 µL of N,O-bis-trimethylsilyl-trifluoroacetamide (BSTFA, Macherey-Nagel, Düren, Germany) was added. Incubation was continued for 30 min. The obtained derivative was analyzed by gas chromatography-mass spectrometry (GC/MS 7890 A, 5975 C quadrupole detector, Agilent Technologies, Santa Clara, CA, USA). The temperature gradient, used for separation, was as follows: 150 °C for 3 min, increased at 8 °C min^{-1} up to 230 °C, and increased at 25 °C min^{-1} up to 325 °C. The trimethylsilyl O-methyloxime derivative of glucose was measured via the ion clusters at *m/z* 554–561 (glucose carbons 1–6) and *m/z* 319–323 (glucose carbons 3–6) (Laine and Sweeley, 1971). Generally, samples were first measured in scan mode to check for potential isobaric interference between analytes and other sample components. The labeling patterns of the analytes of interest were then determined in duplicate using selective ion monitoring (SIM) of the selected ion clusters (Becker et al., 2005). The mean experimental error for mass isotopomer quantification was below 1%. For qualitative inspection of metabolic pathways in ^{13}C experiments, the summed fractional labeling (SFL) (Christensen et al., 2000) of the glucose monomer of glycogen, as well as the SFL of succinate and selected amino acids, was calculated from experimental mass isotopomer distributions, after correcting the data for the natural occurrence of isotopes (van Winden et al., 2002). For the quantitative estimation of intracellular fluxes, experimental mass isotopomer distributions were automatically corrected for the natural occurrence of isotopes, using the software OpenFLUX (Quek et al., 2009).

2.9. Isotopomer network model and calculation of flux distributions

The metabolic network used for flux analysis was adapted from a previous study of *B. succiniciproducens* (Becker et al., 2013). The catabolic pathway for sucrose was based on the repertoire of the related rumen bacterium *M. succiniciproducens*, which uses a sucrose phosphotransferase system (PTS), sucrose 6-phosphate hydrolase, and a fructose PTS for the transport and utilization of sucrose (Lee et al., 2010). Owing to a lack of experimental evidence, a mannose PTS was not considered (Lee et al., 2010).

As described in detail below (Sections 3.4 and 3.5), the basic network draft was substantially refined, extended, and validated for *B. succiniciproducens* based on experimental findings in this study. For the flux calculation, the curated and updated network was implemented into OpenFLUX (Quek et al., 2009), considering all underlying isotopomer carbon transitions. The flux software was adapted for integrated flux estimation from four separate labeling data sets (https://sourceforge.net/projects/openflux). Such an extended data set proved necessary to resolve the fluxes of interest on sucrose. Stoichiometric data on growth and product formation and biomass synthesis together with ^{13}C labeling data were used as input. The measured activity of the malic enzyme was used as upper boundary of the corresponding flux to constrain the model. The set of free fluxes that resulted in minimum deviation between the experimental and simulated labeling data was taken as the best estimate for the in vivo fluxes. Because the non-linear structure of isotopomer models may potentially lead to local minima (Wiechert et al., 1997), multiple parameter initialization was used to investigate whether the obtained flux distribution represented the global optimum. Statistical analysis of the obtained fluxes was conducted by Monte-Carlo analysis and yielded 90% confidence intervals for the flux parameters (Wittmann and Heinzle, 2002).

2.10. Stoichiometric network and elementary flux mode analysis

Computation of elementary flux modes was carried out as described previously (Melzer et al., 2009). The underlying stoichiometric network is given in Table S3. All redox co-factors were considered for stoichiometric balancing, whereas an apparent ATP excess was allowed to account for cellular maintenance (Becker et al., 2013). Redox metabolism comprised two transhydrogenases and NADH dehydrogenase (Kim et al., 2007).

3. Results

3.1. Growth and succinate production of B. succiniciproducens DD1 on sucrose

B. succiniciproducens DD1 achieved a succinate titer of > 150 mM (18.0 g L^{-1}), when grown in anaerobic batch culture on sucrose minimal medium (Fig. 1A). Production occurred at a molar yield of 1 mol mol^{-1} (Table 2). A maximum growth rate of 0.44 ± 0.03 h^{-1} allowed for complete consumption of the sugar within 14 h (Fig. 1A). The relatively low biomass concentration (8 g L^{-1}) and yield [76 (g cell dry mass) (mol sucrose)$^{-1}$] indicated that the dominant fraction of carbon was not used for growth. The most abundant by-product was lactate (8.9 ± 0.1 g L^{-1}). Formate (8.2 ± 0.2 g L^{-1}) and acetate (8.0 ± 0.3 g L^{-1}) accumulated to almost the same level, whereas ethanol (1.6 ± 0.0 g L^{-1}) was formed less. Subsequent analysis of the culture supernatant, using HPLC and NMR, revealed a number of minor by-products, such as pyruvate, fumarate, 2-oxoisovalerate, acetoin, and several amino acids, including alanine, valine, leucine, aspartate, glutamate, and glycine (Table 2). The carbon balance completely closed, which indicated high consistency of the obtained data (Fig. 1B). Towards the final stage of the cultivation, the growth physiology of *B. succiniciproducens* slightly changed (Fig. 1A). After approximately 12 h, lactate and succinate formation further increased at the expense of growth, which was no longer exponential.

3.2. The product spectrum of B. succiniciproducens DD1 is strongly impacted by the carbon source

In a set of experiments, the physiology of sucrose-grown *B. succiniciproducens* was compared to that of cells, grown on the two sucrose monomers. Additional cultures on glucose and fructose were, therefore, conducted (Fig. 2). To allow for direct comparison of the data from the three substrates, the yields in the Fig. 2 are given on a C-molar basis (Buschke et al., 2011). Succinate production was highest on glucose, followed by sucrose and finally fructose. Acetate exhibited a similar

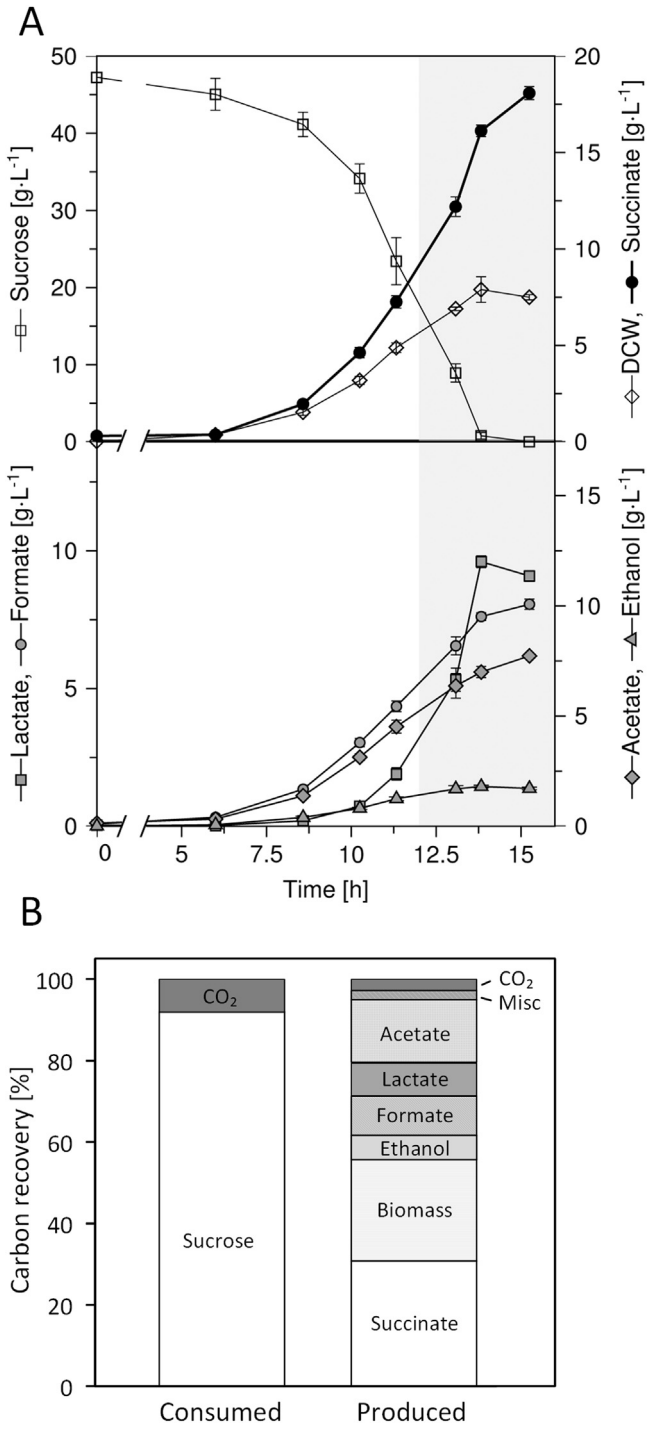

Fig. 1. *Cultivation characteristics of Basfia succiniciproducens DD1 with sucrose as the carbon source, comprising the cultivation profile (A) and the carbon balance (B).* After 12 h, cells shifted from exponential to non-exponential growth and product yields changed (highlighted in grey). The data from the first exponential growth phase were taken into account for ^{13}C metabolic flux analysis (Table 2). The carbon balance considered sucrose and CO_2 as substrates. PEP carboxylation (Fig. 5) was considered as CO_2-consuming reaction. In addition, secreted compounds (Table 2), biomass (Table 2), and CO_2, stemming from the CO_2-forming reactions (Fig. 5) were taken into account as products. The carbon content of the biomass was taken from a previous study (Becker et al., 2013).

trend of production. The opposite trend, i.e., increasing production from glucose to sucrose and fructose, was observed for lactate and ethanol, which is a bit surprising given that all three substrates are structurally similar carbohydrates. Interestingly, the affected by-products all originated from the pyruvate node.

Table 2
Kinetics and stoichiometry of succinate-producing *Basfia succiniciproducens* DD1. The data shown comprise specific growth rate (μ_{max}), sucrose uptake rate (q_s), and yield coefficients for biomass ($Y_{X/S}$) and secreted products ($Y_{Product/S}$) and represent mean values and standard deviations from ten biological replicates.

Yield coefficients				
$Y_{X/S}$	75.7	±	0.6	g mol^{-1}
$Y_{Succinate/S}$	1.01	±	0.02	mol mol^{-1}
$Y_{Formate/S}$	1.26	±	0.01	mol mol^{-1}
$Y_{Acetate/S}$	1.00	±	0.01	mol mol^{-1}
$Y_{Ethanol/S}$	0.38	±	0.01	mol mol^{-1}
$Y_{Lactate/S}$	0.42	±	0.01	mol mol^{-1}
$Y_{Pyruvate/S}$	18.5	±	1.1	mmol mol^{-1}
$Y_{Fumarate/S}$	38.8	±	2.4	mmol mol^{-1}
$Y_{2\text{-}Oxoisovalerate/S}$	3.0	±	1.2	mmol mol^{-1}
$Y_{Acetoin/S}$	10.1	±	4.1	mmol mol^{-1}
$Y_{Alanine/S}$	6.5	±	0.6	mmol mol^{-1}
$Y_{Valine/S}$	2.4	±	0.2	mmol mol^{-1}
$Y_{Glycine/S}$	2.2	±	0.2	mmol mol^{-1}
$Y_{Leucine/S}$	0.5	±	0.1	mmol mol^{-1}
$Y_{Aspartate/S}$	2.2	±	0.1	mmol mol^{-1}
$Y_{Glutamate/S}$	0.3	±	0.0	mmol mol^{-1}
Specific rates				
μ_{max}	0.44	±	0.03	h^{-1}
q_s	5.8	±	0.4	mmol g^{-1} h^{-1}

3.3. The fructose monomer of sucrose is used for glycogen synthesis

Given the surprising finding that the metabolism of sucrose was not simply the additive outcome of its two monomers glucose and fructose, an isotopic study was designed to study the metabolic pathways of sucrose metabolization in more detail. For this purpose, a tracer substrate with two differently labeled subunits, i.e., [$^{13}C_6^{Frc}$] sucrose, was used. *B. succiniciproducens* cells contain glycogen, which is derived from glucose 6-phosphate (Becker et al., 2013). The ^{13}C labeling of glycogen is accessible via GC/MS analysis of its monomer glucose, which offered a direct readout for conversion of each of the two sucrose subunits into intracellular glucose 6-phosphate. The specific ^{13}C enrichment in only the fructose part of the tracer substrate allowed inferring the origin of glycogen, based on its ^{13}C enrichment, i.e. the summed fractional labeling (SFL). The exact relative contribution of each the two subunits could be deduced from the experimental SFL through linear interpolation, as described before (Wittmann et al., 2004). The value observed for the given experimental set-up (SFL = 0.26) and parallel studies on other sucrose tracers (Table 3) revealed that a surprisingly high amount (25–30%) of the glucose 6-phosphate pool stemmed from the fructose subunit of sucrose. The supposed PTS mediated uptake of fructose with carbon withdrawal towards the lower glycolysis should, however, have resulted in a much lower contribution (Wittmann et al., 2004). This was the second finding that indicated a different sucrose utilization pathway in *B. succiniciproducens*. A first insight into this pathway was obtained from closer inspection of the individual mass isotopomers of glycogen-derived glucose (Fig. 3A). The presence of a significant fraction of [$^{13}C_6$] monomers in glycogen (M+6) indicated that intact fructose units entered the glucose 6-phosphate pool without further rearrangement of the carbon skeleton.

3.4. Fructokinase is a functional enzyme in sucrose-grown B. succiniciproducens

Based on the observed labeling pattern, direct phosphorylation of fructose into fructose 6-phosphate by fructokinase emerged as so far undescribed route in *B. succiniciproducens*. Fructokinase activity was observed in cell extracts of *B. succiniciproducens* DD1, grown on minimal sucrose medium (Fig. 4). The maximum specific activity of the ATP-dependent enzyme was 67 ± 3 mU mg^{-1}. It turned out that elevated amounts of Mg^{2+} were needed to fully activate the enzyme. Kinetic analysis of fructokinase revealed a high substrate affinity for both

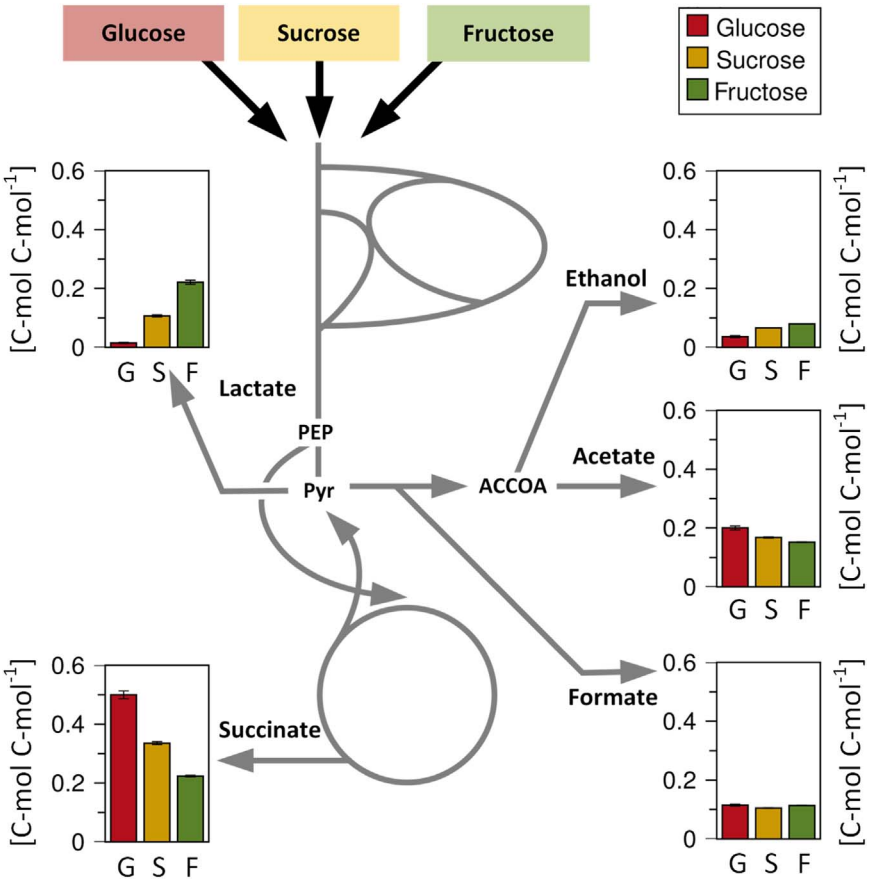

Fig. 2. Growth and production stoichiometry of *Basfia succiniciproducens* DD1 on glucose (G), fructose (F), and sucrose (S) as the carbon source. For comparison, the product yields are given in C-mol C-mol^{-1}. The data for glucose (red), sucrose (yellow), and fructose (green) represent mean values and standard deviations from at least three biological replicates and are placed into the graphical representation of the metabolic network of *B. succiniciproducens* to link the respective products to their precursors. PEP: phosphoenolpyruvate, PYR: pyruvate, ACCOA: acetyl coenzyme A, OAA: oxaloacetate.

Table 3
Summed fractional labeling (SFL) of the glucose monomer of glycogen from isotope experiments with *Basfia succiniciproducens* DD1 on different sucrose tracers. The SFL was obtained via GC-MS analysis of the trimethylsilyl derivative of the glucose monomer of glycogen at *m/z* of 554–560, involving correction for natural isotopes. The relative contribution of the glucose and fructose subunit of sucrose to the glucose 6-phosphate pool was estimated as described previously (Wittmann et al., 2004).

Tracer substrate	Exp. SFL			From glucose [%]			From fructose [%]		
[1-$^{13}C^{Glc}$] sucrose	0.13	±	0.0	74	±	0	26	±	0
[1-$^{13}C^{Frc}$] sucrose	0.06	±	0.0	69	±	1	31	±	1
[$^{13}C_6^{Frc}$] sucrose	0.26	±	0.1	74	±	2	26	±	1
Average				**72**	±	**3**	**28**	±	**2**

fructose (K_M = 0.22 ± 0.03 mM) and ATP (K_M = 0.14 ± 0.01 mM). Obviously, fructokinase (E.C. 2.7.1.4) is a functional enzyme in *B. succiniciproducens*. It is expressed in sucrose-grown cells and, therefore, might be used by the organism during sucrose metabolization.

3.5. Enzymatic repertoire at the pyruvate node

A set of enzymatic assays was now conducted in order to explore the presence of selected enzymes around the pyruvate node. *B. succiniciproducens* exhibited high activity of PEP carboxykinase, lactate dehydrogenase, pyruvate kinase, and PEP carboxylase (Table 4). Malic enzyme and isocitrate dehydrogenase showed much lower activity, but both enzymes were expressed during growth on sucrose, potentially suggesting their contribution to NADPH formation and to the functional operation of the oxidative branch of the TCA cycle. All enzymes were considered in the metabolic network for subsequent metabolic flux analysis (Fig. 5). In addition, an isotope experiment verified that pyruvate formate lyase was reversible, whereas pyruvate dehydrogenase was irreversible under the conditions studied (see supplement), similar to previous observations in the relative microbe *Actinobacillus succinogenes* (McKinlay and Vieille, 2008).

3.6. The reductive TCA cycle is the dominant pathway to succinate

In *A. succinogenes*, a production of succinate through the oxidative branch of the TCA cycle can be excluded, because the organism does not possess the necessary enzymes, as reflected by its glutamate auxotrophy (McKinlay et al., 2005). In contrast, *B. succiniciproducens* can produce succinate via the oxidative and via the reductive TCA cycle. Both fluxes were resolved by a tracer experiment with all available CO_2, labeled as $^{13}CO_2$ (Fig. 3B). As shown from the experimental succinate labeling, the reductive route clearly was the dominant pathway. The M +1 mass isotopomer of succinate, specific for this route, displayed the major fraction (89%), whereas the fraction of non-labeled (M+0) succinate, i.e., the upper boundary of the relative flux through the oxidative branch, was rather small (5%). A significant fraction (11%) of double labeled (M+2) succinate was also attributed to the reductive pathway and additionally revealed that carboxylation of PEP in *B. succiniciproducens* is reversible, which was implemented into the metabolic network accordingly.

3.7. Four parallel ^{13}C labeling experiments with analysis of 460 individual mass isotopomers resolve intracellular fluxes on sucrose

A central aim of this study was the quantitative analysis of the carbon metabolism of *B. succiniciproducens* on the level of intracellular fluxes. The previous knowledge and the new findings in this work provided a refined and validated network of the carbon core

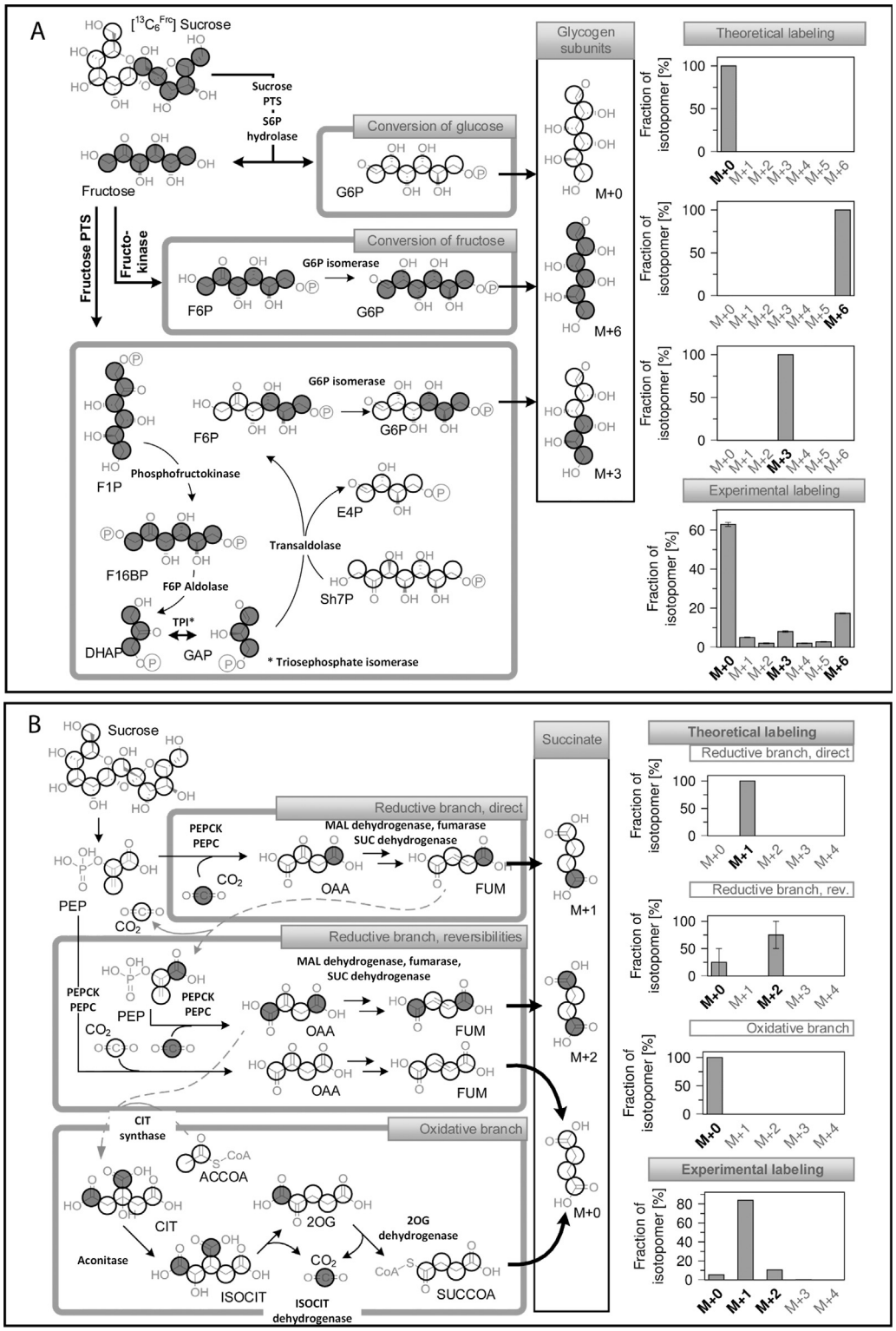

Fig. 3. Resolution of metabolic fluxes in *Basfia succiniciproducens* DD1 by isotope experiments. Flux partitioning between fructokinase and the fructose PTS assessed from a culture grown on [$^{13}C_6^{Frc}$] sucrose (A). The chosen tracer substrate results in a different labeling pattern of glucose 6-phosphate, which can be monitored via the glucose monomer of cellular glycogen, formed from this sugar phosphate. ATP-dependent phosphorylation of fructose by fructokinase yields fructose 6-phosphate and intact (M +6) labeled glycogen units. In contrast, PEP-dependent phosphorylation yields fructose 1-phosphate and (M+3) labeled glycogen units. The experimental labeling of glycogen-derived glucose exhibits both mass isotopomers and unravels the simultaneous contribution of both pathways to sucrose catabolism. Flux partitioning between the reductive and oxidative TCA cycle from a culture on $^{13}CO_2$ and naturally labeled sucrose (B). Succinate, produced from $^{13}CO_2$ and naturally labeled sucrose through the reductive branch, is single labeled, owing to incorporation of $^{13}CO_2$ in the underlying carboxylation step. Scrambling of the label at the level of the symmetric molecules of fumarate and succinate, together with reversible carboxylation can, additionally, form double labeled (M+2) succinate. In contrast, the oxidative TCA cycle branch leads to loss of ^{13}C and exclusively yields naturally labeled succinate. Naturally labeled succinate can, through a combination of different reactions, also result from the reductive part, so that the (M+0) mass isotopomer fraction—in this simplified view—indicates the upper boundary for contribution of the oxidative route. G6P: glucose 6-phosphate, F6P: fructose 6-phosphate, F16BP: fructose 1,6-bisphosphate, E4P: erythrose 4-phosphate, Sh7P: sedoheptulose 7-phosphate, DHAP: dihydroxyacetone phosphate, GAP: glyceraldehyde 3-phosphate, 3PG: 3-phosphoglycerate, PEP: phosphoenolpyruvate, PYR: pyruvate, ACCOA: acetyl coenzyme A, OAA: oxaloacetate, CIT: citrate, ISOCIT: isocitrate, 2OG: 2-oxoglutarate, SUCCOA: succinyl coenzyme A, FUM: fumarate, MAL: malate, PTS: phosphotransferase system.

metabolism of *B. succiniciproducens* (Fig. 5). The topology of the metabolism with various parallel, reversible and bidirectional reactions and pathways, required a comprehensive strategy to resolve the intracellular flux distribution. We conducted four parallel tracer studies on (i) [1-$^{13}C^{Glc}$] sucrose and naturally labeled CO_2, (ii) [$^{13}C_6^{Frc}$] sucrose and naturally labeled CO_2, (iii) an equimolar mixture of [$^{13}C_{12}$] sucrose and naturally labeled sucrose, plus naturally labeled CO_2, and (iv) $^{13}CO_2$, $MgCO_3$, and naturally labeled sucrose, the latter labeling all available CO_2. From the tracer cultivations, the ^{13}C labeling of amino acids from the cellular protein, of glucose from cellular glycogen, and of secreted succinate, was measured. This provided sensitive data to estimate the free flux parameters of interest. For example, the use of [1-$^{13}C^{Glc}$] sucrose allowed us to quantify the flux partitioning ratio between the Embden-Meyerhof-Parnas (EMP) and pentose phosphate (PP) pathways at the glucose 6-phosphate node (Wittmann et al., 2004). The reversibility of glucose 6-phosphate isomerase, needed for precise estimation of the flux split at the node (Wittmann and Heinzle, 2001), was accessible via the ^{13}C labeling pattern of the glucose 6-phosphate

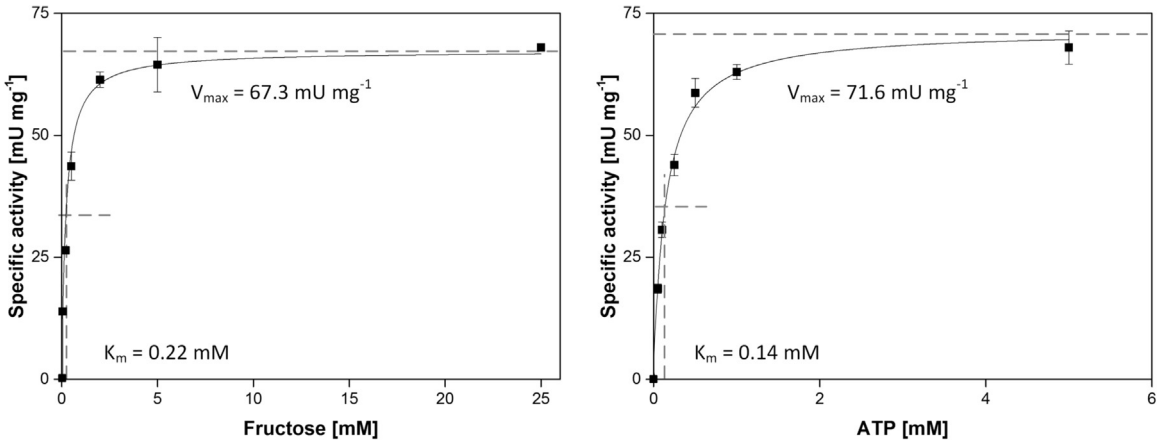

Fig. 4. *In vitro* activity and kinetic properties of fructokinase in crude cell extract of sucrose-grown *Basfia succiniciproducens* DD1. The K_M value for fructose was assessed with 1 mM ATP (A). The K_M value for ATP was determined with 25 mM fructose (B).

Table 4
Enzymatic repertoire of sucrose-grown *Basfia succiniciproducens* DD1 around the pyruvate node. The data represent mean values and standard deviations from three replicates.

Enzyme	Activity [mU/mg]		
Lactate dehydrogenase	1658	±	23
Pyruvate kinase	1598	±	188
Malic enzyme	54	±	1
PEP carboxylase	854	±	52
PEP carboxykinase[a]	2498	±	251
Isocitrate dehydrogenase	6	±	0

[a] The activity of PEP carboxykinase was measured in cell-free extracts of a Δ*ldhA* deletion strain, because for the wild type, a potentially falsifying background resulting from PEP conversion into pyruvate and then into lactate via highly active pyruvate kinase and lactate dehydrogenase appeared likely.

pool through the analysis of glycogen (McKinlay et al., 2007; McKinlay and Vieille, 2008). The differentiation between the newly discovered pathways of fructose-phosphorylation was achieved by the combination of [$^{13}C_6^{Frc}$] sucrose as a tracer substrate and ^{13}C labeling analysis of glycogen-derived glucose (Fig. 3A). The flux partitioning between the oxidative and reductive branch of the TCA cycle was determined by the combination of $^{13}CO_2$ and naturally labeled sucrose, which results in pathway specific labeling patterns for succinate as described in the supplement (Fig. 3B).

Based on this strategy, *B. succiniciproducens* was cultivated as follows: the above-specified four different isotope experiments were conducted together with six further non-labeled biological replicates to additionally assess growth kinetics and stoichiometry. Metabolic flux analysis, as applied here, requires a metabolic and isotopic steady-state of the investigated culture (Becker et al., 2008). Metabolic steady-state was ensured from constant growth and production behavior (Fig. S2A), exemplified for different metabolites from the parallel tracer studies, sampled at different time points of the cultivation; ^{13}C labeling patterns remained constant over time (Fig. S2B). Hereby, it should be noted that the flux studies were sampled and analyzed during the steady-state, before the late shift in growth behavior (Fig. 1A) had started. The labeling analysis of all isotope experiments provided 460 individual mass isotopomers to be explored for metabolic flux analysis (Fig. S3). An initial qualitative inspection of the labeling data confirmed that the fructose subunit of sucrose is re-cycled to the glucose 6-phosphate pool. The SFL of glycogen-derived sucrose from the different tracer studies consistently quantified the relative contribution from fructose to approximately 25–30%, whereas the remaining 70–75% originated from the glucose monomer of the substrate (Table 3). In addition, the occurrence of (M + 6) mass isotopomers in the glucose monomer of glycogen showed the in vivo activity of fructokinase (Fig. 3A).

3.8. Distribution of central carbon fluxes in sucrose-grown B. succiniciproducens

The extensive data set was now used to determine the intracellular fluxes in *B. succiniciproducens*. The calculation of the metabolic fluxes considered the measured growth and the product formation (Table 2), the anabolic demand for biomass precursors (Table S2), and the ^{13}C labeling data from the parallel isotope studies (Fig. S3), which were all integrated for the flux calculation. The set of intracellular fluxes that gave minimum deviation between experimental and simulated labeling patterns was taken as the best estimate for the intracellular flux distribution (Fig. 6). As indicated by the high accordance of experimental and simulated labeling patterns, an excellent fit of all four parallel labeling data sets to the model was achieved (Fig. S3). The average deviation between experimental and simulated labeling patterns was below 1%. Multiple flux calculations with randomly varied initialization values for the flux parameters yielded identical results, confirming that the global minimum was identified. Statistical evaluation provided very narrow confidence intervals for the single flux parameters, indicating that the fluxes were determined at high precision (Fig. 6).

3.8.1. Both fructose PTS and fructokinase contribute to phosphorylation of the fructose subunit of sucrose

A fraction of intracellular fructose was transiently exported, possibly into the periplasm (no fructose was detected in culture supernatant), and was then re-assimilated through the fructose PTS (Fig. 6). The remaining fraction of free fructose was phosphorylated by fructokinase and entered the central metabolism at the level of fructose 6-phosphate. The reversible nature of phosphoglucoisomerase then resulted in the observed transfer of intact fructose units towards glucose 6-phosphate and then into the glycogen pool (Table 3).

3.8.2. The PP pathway mainly provides precursors for biomass

During the further metabolization, carbon was mainly channeled through the EMP pathway. Only a small flux entered the oxidative PP pathway, where it was almost completely consumed to supply erythrose 4-phosphate and ribose 5-phosphate as anabolic precursors. The PP pathway flux did not exceed the anabolic demand, so that there was almost no back flux of carbon from the PP pathway into glycolysis. Starting from glucose 6-phosphate, the EMP pathway flux increased gradually through co-entry of fructose units at the level of fructose 6-phosphate and fructose 1,6-bisphosphate. At the glyceraldehyde 3-phosphate node, almost the entire carbon was channeled further down the glycolytic chain, except for a low back flux through the reversible reactions of the PP pathway.

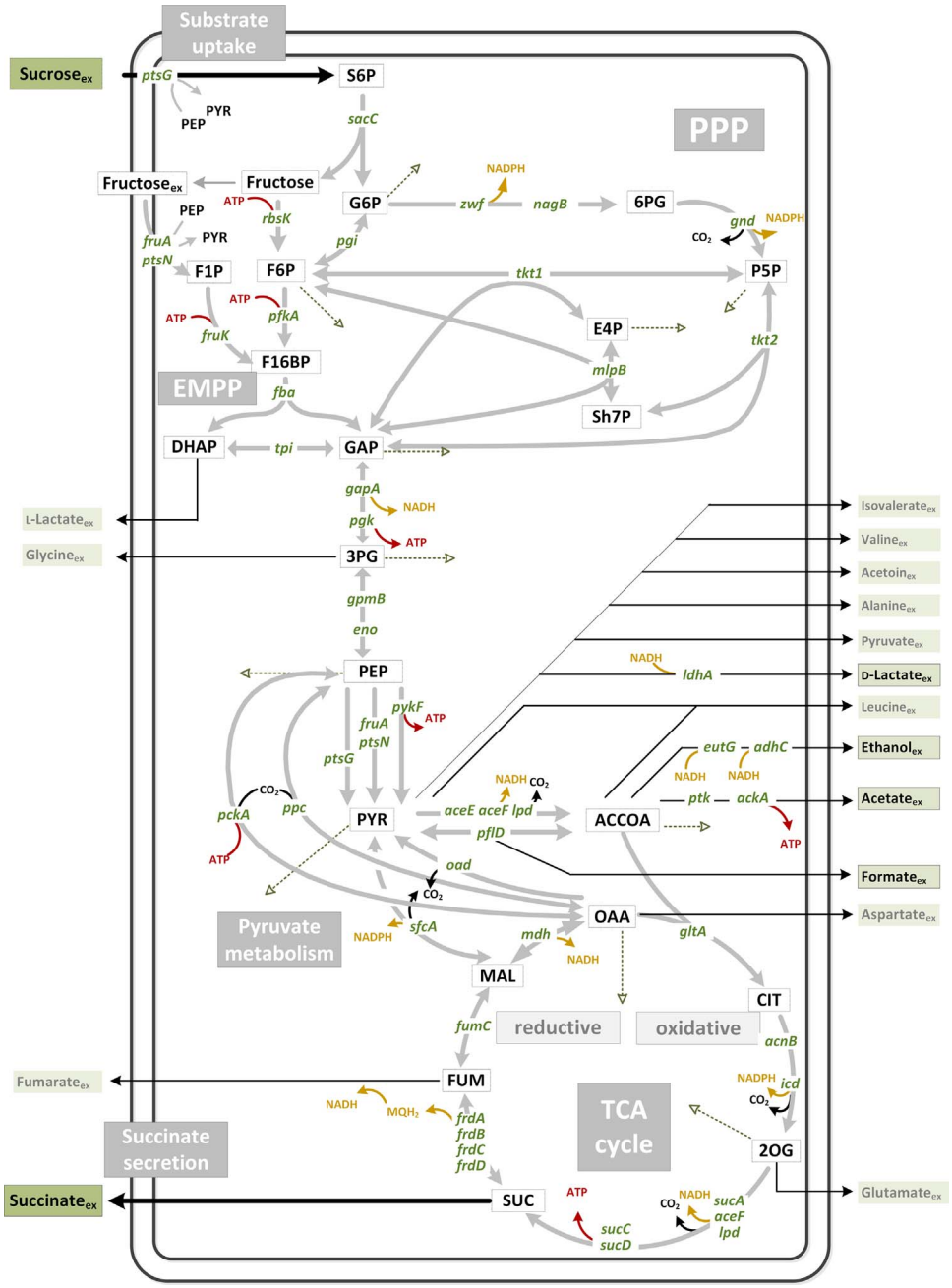

Fig. 5. Validated and curated metabolic network of the central carbon metabolism of sucrose-grown *Basfia succiniciproducens* DD1. Pathways for metabolization of sucrose leading to succinate and main by-products (light green, black text), as well as additional by-products (light green, grey text), detected in this study. Encoding genes (green), redox cofactors (yellow), and energy metabolites (red) are displayed. Dotted arrows indicate anabolic reactions into biomass. S6P: sucrose 6-phosphate, G6P: glucose 6-phosphate, F1P: fructose 1-phosphate, F6P: fructose 6-phosphate, F16BP: fructose 1,6-bisphosphate, 6PG: 6-phosphogluconate, P5P: pentose 5-phosphate, E4P: erythrose 4-phosphate, Sh7P: sedoheptulose 7-phosphate, DHAP: dihydroxyacetone phosphate, GAP: glyceraldehyde 3-phosphate, 3PG: 3-phosphoglycerate, PEP: phosphoenolpyruvate, PYR: pyruvate, ACCOA: acetyl coenzyme A, OAA: oxaloacetate, CIT: citrate, 2OG: 2-oxoglutarate, SUC: succinate, FUM: fumarate, MAL: malate, AD(T)P: adenosine di(tri)phosphate, NAD(P)H: nicotinamide adenine dinucleotide (phosphate), reduced, MQH_2: menaquinone, reduced, PPP: pentose phosphate pathway, TCA cycle: tricarboxylic acid cycle, EMPP: Embden–Meyerhof–Parnas pathway.

3.8.3. Three parallel enzymes convert PEP into pyruvate: the PTS systems for sucrose and fructose and pyruvate kinase

At the level of PEP, carbon was converted either to oxaloacetate towards the desired product succinate or to pyruvate, which mainly caused carbon loss into by-products. Inherently linked to the uptake of sucrose, the sucrose PTS was the major enzyme that formed pyruvate from PEP. In addition, the fructose PTS and, to a minor but significant extent, pyruvate kinase, caused loss of PEP. The concerted action of the different enzymes resulted in a significant influx into the pyruvate pool, where it triggered the formation of elevated levels of by-products such as lactate, ethanol, formate, and acetate.

3.8.4. Malic enzyme is active in vivo and withdraws carbon from the succinate production pathway

Oxaloacetate was generated from PEP by carboxylation, matching a flux of 95%. However, the valuable precursor was not fully converted into succinate. In fact, malic enzyme was found to recycle carbon back to pyruvate (28%). The contribution of malic enzyme was significant. The enzyme supplied almost one quarter of the total influx into the pyruvate pool. In addition, a minor flux was also attributed to oxaloacetate decarboxylase (4%).

3.8.5. Succinate is exclusively formed by the reductive TCA cycle branch

The oxidative branch of the TCA cycle exclusively served as an anabolic route. The flux matched with the anabolic demand for 2-oxoglutarate as a precursor for amino acids of the glutamate family. No succinate was formed through this branch. The low flux corresponded to a low in vitro activity for isocitrate dehydrogenase (Table 4). Accordingly, succinate was completely provided by the reductive route. Taken together *B. succiniciproducens* channeled a flux of > 50% into the desired product, which equaled a yield of > 1 (mol succinate) (mol sucrose)$^{-1}$. The production pathway could not handle the entire flux, but exhibited a slight overflow formation of fumarate.

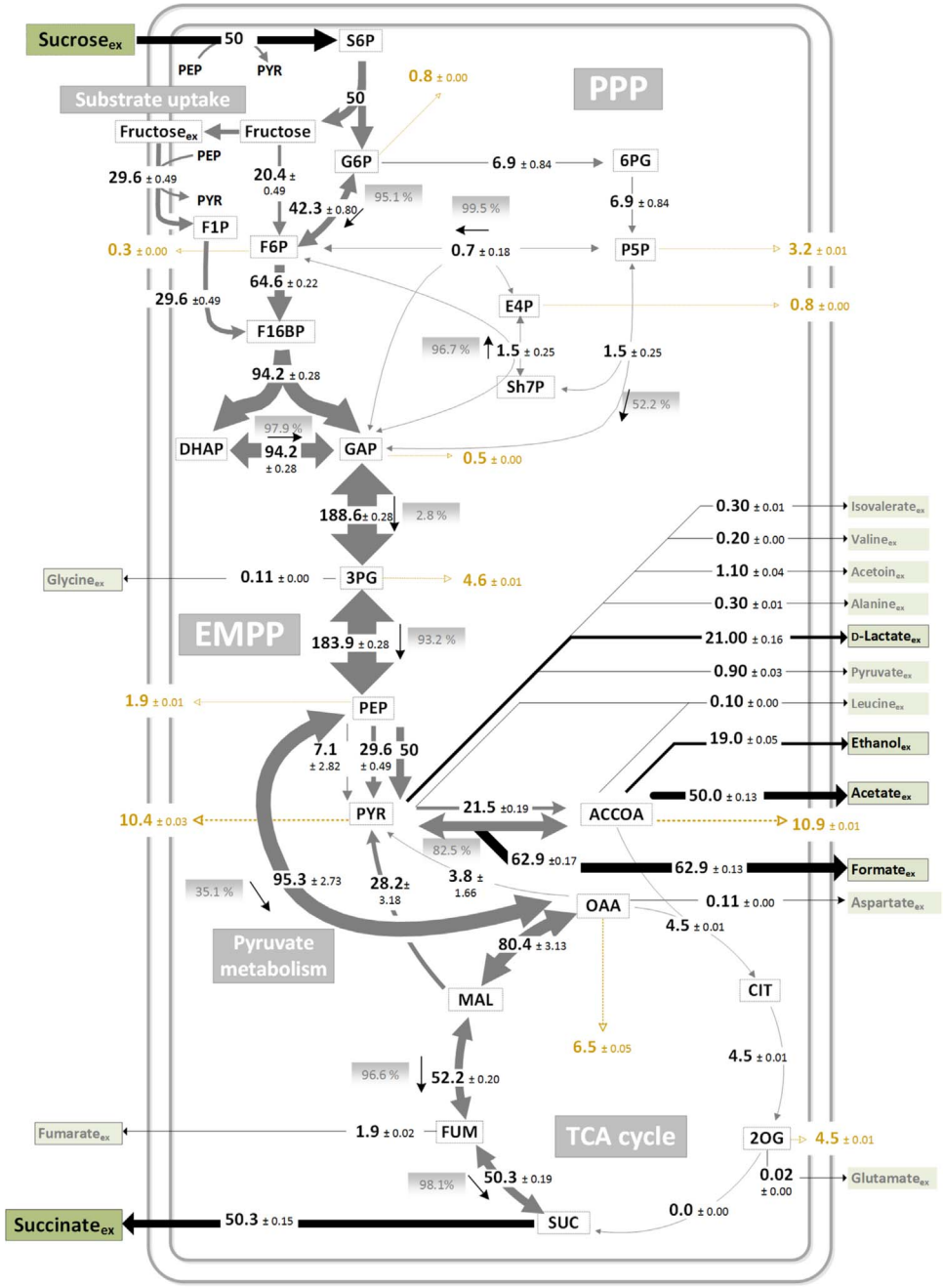

Fig. 6. Intracellular carbon fluxes of *Basfia succiniciproducens* DD1 on sucrose as determined by ^{13}C metabolic flux analysis. The direction of net flux is indicated by a black arrow. Flux reversibility (grey boxes, white text) is given in percent, whereby 100% represents infinitely high reversibility and 0% represents an irreversible reaction. Fluxes into biomass are given in yellow, whereas black arrows indicate carbon influx and efflux. All fluxes are given as a molar percentage of the mean specific glucose uptake rate of $q_{Suc} = 5.8$ mmol g^{-1} h^{-1}, which was set to 50%. This equals the common format of 100% hexose uptake and facilitates the comparison with flux data on monosaccharides.

3.9. Metabolic engineering of *B. succiniciproducens* for enhanced succinate production

3.9.1. Deletion of the fructose PTS

As demonstrated, *B. succiniciproducens* DD1 operated the fructose PTS to phosphorylate fructose in a PEP-dependent manner (Fig. 6). The inherent utilization of PEP by this type of phosphorylation is generally undesirable for succinate production. The deletion of the fructose PTS appeared, therefore, beneficial to re-direct the formed intracellular fructose to the newly discovered fructokinase. The *fruA* gene, encoding for the fructose specific component of the fructose PTS, was, hence, deleted from the genome. The desired mutation in clones, obtained after the second recombination, was verified by PCR using the corresponding primer pair $PR_{fruA}1$ and $PR_{fruA}4$ (Table S1). Positive clones were identified by a fragment size of 2100 bp, which was 1600 bp shorter than that observed for the wild type (3700 bp), as expected. The derived strain *B. succiniciproducens* DD1 Δ*fruA* was then characterized for its production properties in sucrose-grown batch cultures. Most strikingly, the succinate yield was increased by 44% to 1.45 mol (mol sucrose)$^{-1}$ in the novel mutant. In addition, the level of pyruvate-derived by-products was substantially decreased: lactate formation was reduced by 68% and formate formation was reduced by 17% (Fig. 7A). In addition, the ethanol level was reduced by 58% (from 0.40 to 0.17 mol mol^{-1}).

3.9.2. Overexpression of fructokinase

The discovered fructokinase (*rbsK*) was a promising amplification target to enhance the natural activity of the enzyme and reduce fructose phosphorylation at the expense of PEP. The gene *rbsK* was overexpressed in an episomal plasmid under the control of the strong native *ackA* promoter. The overexpression of the gene was evaluated by determining the specific fructokinase activity in the designated strain *B. succiniciproducens* DD1 P_{ackA}*rbsK*. This was increased about threefold to 200 mU mg^{-1} (Table 5) in the mutant in comparison to that in the wild

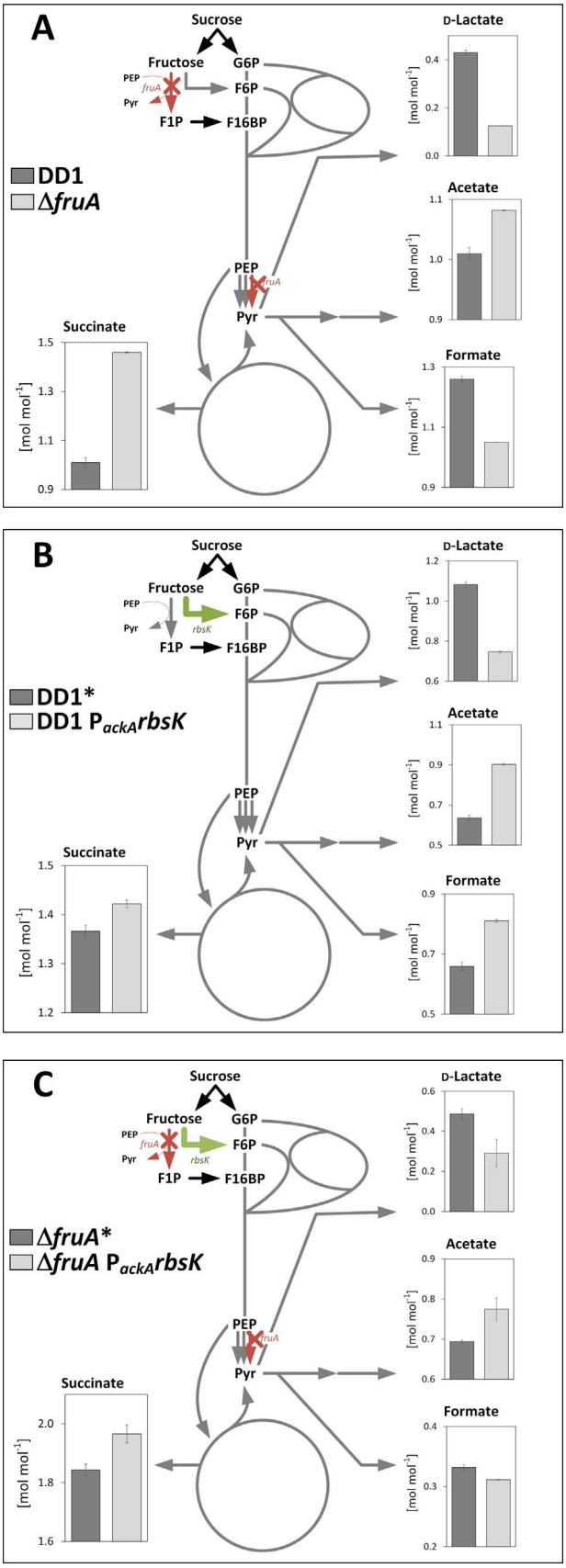

Fig. 7. Systems metabolic engineering of *Basfia succiniciproducens* DD1 for succinate production. Impact of the deletion of the fructose PTS (*fruA*) (A), the amplification of fructokinase (*rbsK*) (B), and the combined deletion of *fruA* and amplification of *rbsK* on production performance (C). The designation of the strains refers to Table 1.

Table 5
Specific activity of fructokinase in *Basfia succiniciproducens* DD1*, DD1 P_{ackA}*rbsK*, Δ*fruA**, and Δ*fruA* P_{ackA}*rbsK* grown on sucrose. Data represent mean values and standard deviations from three replicates.

Strain	Specific activity [mU/mg]
DD1*	67 ± 3
DD1 P_{ackA}*rbsK*	200 ± 11
Δ*fruA**	50 ± 4
Δ*fruA* P_{ackA}*rbsK*	154 ± 8

type DD1 and the control strain DD1*, which carried the empty plasmid. Clearly, the fructokinase mutant exhibited improved production performance (Fig. 7B). The succinate yield was increased by 4%, whereas lactate formation was reduced by 31%. Acetate and formate levels were slightly increased, whereas ethanol was not produced by either of the two strains.

3.9.3. Combination of beneficial modifications

Further, the two beneficial modifications were combined to investigate potential synergistic effects. The double mutant DD1 Δ*fruA* P_{ackA}*rbsK*, lacking the fructose PTS and overexpressing fructokinase, had about threefold increased fructokinase activity (154 mU mg^{-1}) (Table 5) and produced succinate at a higher efficiency than the parent strain DD1* Δ*fruA* (Fig. 7C): the succinate yield was increased by 6%. Again, by-products were substantially decreased. Lactate formation was reduced by 40% and formate formation was reduced by 5%. Ethanol production was completely abolished in both strains.

3.10. Fed-batch production of succinate from sucrose

Finally, the performance of the engineered sucrose catabolism was evaluated in an industrial fed-batch environment. *B. succiniciproducens* Δ*fruA* was selected for this purpose, because this mutant did not require the addition of an antibiotic. The process involved a sucrose-based medium with an initial batch phase, followed by linear sucrose feeding, upon depletion of the carbon source. *B. succiniciproducens* Δ*fruA* achieved a final succinate titer of 71 g L^{-1}, which was 12% higher than that achieved by the wild type (62 g L^{-1}). In addition, by-product formation was much weaker. For example, the mutant secreted only 7.3 g L^{-1} lactate; the parent strain, 9.3 g L^{-1}. Similarly, formate production was reduced (Fig. 8). The fed-batch fermentation comprised three phases with different product spectra: an initial batch-phase, a substrate-limited feed phase, and a substrate-accumulating phase towards the end of the process. In particular, the two phases with substrate excess resulted in an enhanced succinate yield in the Δ*fruA* strain.

3.11. Computational modeling of succinate production from sucrose

In order to better understand the role of fructokinase from the genomic context, a set of computational simulations was conducted, using elementary flux mode analysis. Hereby, different scenarios were compared. In addition to the real pathway repertoire of the microorganism with the fructose PTS and the newly discovered fructokinase (1), two theoretical topologies helped to understand the role of both enzymes for succinate production. One assumed the absence of fructokinase (2), and the other lacked both the fructose PTS and fructokinase (3). Each calculation provided several thousand elementary flux modes with different efficiency regarding succinate and biomass formation (Fig. 9), to be explored below in close relation to the properties of the wild type and the created mutants.

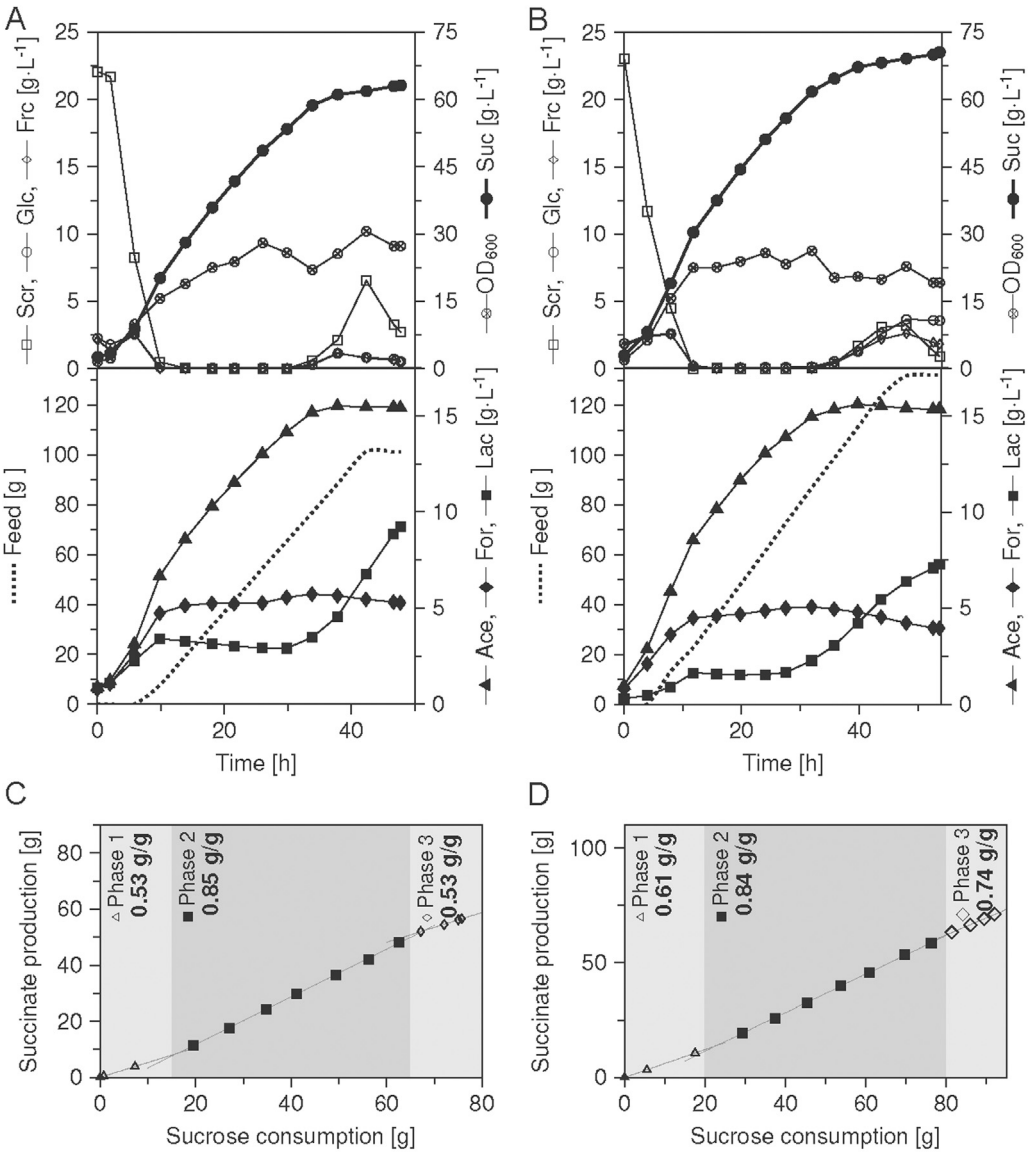

Fig. 8. Fed-batch production of succinate from sucrose by *Basfia succiniciproducens* DD1 (A, C) and the engineered mutant DD1 *ΔfruA* (B, D). After an initial batch phase, a linear feeding strategy was applied. Scr: sucrose, Glc: glucose, Frc: fructose, Suc: succinate, Ace: acetate, Lac: lactate, For: formate.

4. Discussion

4.1. Succinate production from sucrose benefits a from supporting pathway repertoire in substrate uptake and metabolization

One of the most important criteria regarding the efficiency of succinate production is the product yield. Our data provide a detailed insight into the pathways of sucrose metabolism and their impact on the production efficiency. As demonstrated, the sugars tested, i.e. glucose, sucrose, and fructose, strongly affected growth and production performance of *B. succiniciproducens* (Fig. 2). We show that this is due to differences in substrate utilization. Glucose uptake and phosphorylation in *B. succiniciproducens* is ATP-dependent, similar to the related rumen bacterium *M. succiniciproducens* (Becker et al., 2013; Lee et al., 2005, 2006). In contrast, PTS-systems are involved in fructose and sucrose uptake (Lee et al., 2006), which inherently couples substrate uptake and phosphorylation to the formation of pyruvate from PEP. This explains the pronounced accumulation of pyruvate-derived by-products on fructose and sucrose as carbon source, respectively. However, it does not explain why the two PTS-sugars differ so much from each other. In fact, PTS-mediated phosphorylation of both sucrose subunits, as shown for *M. succiniciproducens* (Lee et al., 2010), provides the same amount of pyruvate on sucrose as that on fructose so that the product spectrum of sucrose-grown cells of *B. succiniciproducens* should have resembled that on fructose. This was clearly not the case. The succinate yield was almost 40% higher on sucrose than on fructose and the by-product formation was much weaker. The sucrose-specific product spectrum and the ^{13}C flux data then led to the discovery of an active fructokinase in *B. succiniciproducens* and a unique way to metabolize sucrose, which differs from that of other succinate-producing rumen bacteria (Lee et al., 2010).

From the viewpoint of microbial physiology, fructokinase might provide a benefit for the bacterium in its native environment. As shown, it enables *B. succiniciproducens* to convert sucrose into succinate in a more efficient manner. Sucrose makes up nearly 50% of grass (da Silva and Arrabaca, 2004)—a typical ingredient of cattle diet—thus rendering it a relevant carbon source in vivo. For the symbiotic existence between succinate-metabolizing propionic acid bacteria and the propionic-acid-consuming cattle host (Guettler et al., 1999), succinate production might be more advantageous for *B. succiniciproducens* than lactate production. The utilization of the ATP-dependent fructokinase instead of a PEP-dependent PTS is a way to increase succinate and decrease lactate production, when sucrose is the carbon source.

From the viewpoint of industrial production, the contribution of the newly discovered fructokinase to phosphorylation of free intracellular fructose beneficially changes the flux at the PEP node: the flux into the

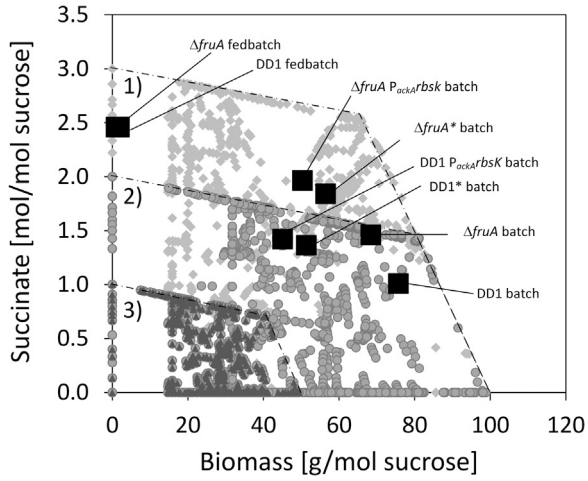

Fig. 9. Model-based evaluation of sucrose-based succinate production in *Basfia succiniciproducens*. The phenotypes of the wild type and engineered production mutants were studied by integration of their performance into the theoretical flux space, derived *in silico* by elementary flux mode analysis. The respective flux space was determined for different scenarios. In addition to the active pathway repertoire of the microorganism with the fructose PTS and newly discovered fructokinase (1), two theoretical topologies helped to understand the role of key enzymes for succinate production. One assumed the absence of fructokinase (2), and the other lacked both the fructose PTS and fructokinase (3). The experimental production properties refer to serum flask batch cultures (Fig. 7A-C) and to the substrate-limited part of the feed phase (phase II) of the fed-batch process (Fig. 8).

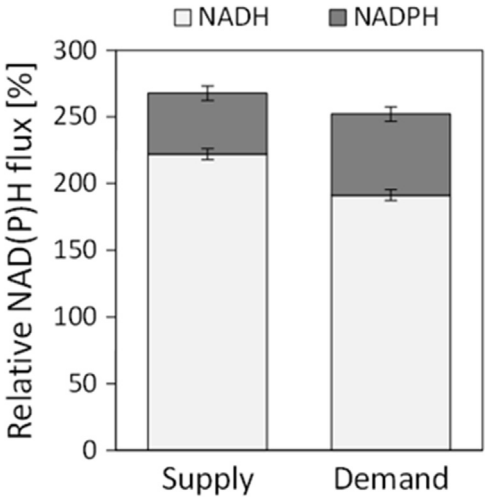

Fig. 10. Redox balance of *Basfia succiniciproducens* DD1 on sucrose. The supply and demand of NADH and NADPH was calculated from the metabolic flux distribution and corresponding requirements for biomass formation. *B. succiniciproducens* was assumed to possess a NADH dehydrogenase for electron transfer from NADH to menaquinone (Kim et al., 2009). The data reflect mean values and 90% confidence intervals from Monte-Carlo simulations.

pyruvate node is reduced so that the cells channel more carbon from PEP towards succinate (Fig. 6). This explains the significantly higher yield on sucrose than on fructose (Fig. 1B). Based on the high yield and the high specific sucrose uptake rate, *B. succiniciproducens* achieved in a remarkable productivity of approximately 6 mmol g^{-1} h^{-1} (Table 2). Most important, the flux data suggested novel genetic targets for enhanced succinate production, namely, the overexpression of fructokinase, the elimination of the fructose PTS, and a combination of the two. The constructed mutants with these modifications revealed strongly enhanced succinate yield and titer, so that the identified targets display valuable features for industrial succinate production.

4.2. Flux partitioning in sucrose metabolization impacts the spectrum of by-products and the generation of ATP

Another important issue in industrial succinate production relates to the supply of ATP and redox power. In sucrose-grown *B. succiniciproducens*, the availability of the main electron acceptor fumarate is reduced, compared to that in glucose-grown bacteria. This directly results from the enhanced flux from PEP to pyruvate, which is owing to the contribution of the fructose PTS and the sucrose PTS to substrate phosphorylation (Fig. 6). Consequently, sucrose-grown *B. succiniciproducens* needs to recycle NAD^+ by other means. This is why ethanol and lactate yields are significantly higher on sucrose than on glucose. This redox-forced flux shift also affects reactions involved in ATP generation. By decreasing the availability of PEP, PEP carboxykinase cannot act efficiently and less succinate can be produced, which is a way for *Pasteurellaceae* to generate ATP (McKinlay et al., 2007; McKinlay and Vieille, 2008). Furthermore, acetyl-CoA is used largely for NAD regeneration through ethanol production, so that less acetate can be generated, which also yields ATP. Nevertheless, ATP availability is probably better on sucrose than on glucose, because the assimilation of a single glucose molecule involves two ATP molecules. During sucrose-uptake, in contrast, only one ATP or PEP is required per hexose. This might explain the fast growth on sucrose (Table 2). On fructose, a purely PTS-consumed carbon source, these effects seem even more extreme. Although only indirect evidence can be presented at this point, the shift from succinate to lactate production seems likely linked to the way of substrate phosphorylation (Fig. 1B). Similarly, *M. succiniciproducens* reveals increased lactate and decreased succinate production on fructose (Lee et al., 2002). A more systematic analysis of succinate production on sucrose, glucose, and fructose in *A. succinogenes* and *M. succiniciproducens* would be interesting to better understanding the underlying differences in the cellular biochemistry and physiology.

4.3. The flux data allow for a detailed inspection of redox metabolism

The complete resolution of metabolic fluxes allows a detailed quantitative inspection of the redox metabolism of *B. succiniciproducens* (Fig. 10). The reactions that supply NADH are glyceraldehyde 3-phosphate dehydrogenase, pyruvate dehydrogenase, and 2-oxoglutarate dehydrogenase. Based on the flux data (Fig. 6) and previous analyses of cofactor specificity (Becker et al., 2013), glucose 6-phosphate dehydrogenase, 6-phosphogluconate dehydrogenase, malic enzyme, and isocitrate dehydrogenase are NADPH-supplying reactions. The intracellular reactions involved in NADH consumption comprised alcohol dehydrogenase, lactate dehydrogenase, malate dehydrogenase, and fumarate reductase. It was further assumed that *B. succiniciproducens* possesses an NADH dehydrogenase for electron transfer from NADH to menaquinone (Kim et al., 2009). Consumption of menaquinone was, hence, regarded as NADH consumption. NADPH is required for growth and its demand results from the determined biomass formation (Table 2) and cellular composition (Table S2). The dominating redox equivalent cofactor was NAD(H), which accounted for 70–80% of the total redox flux. The total redox balance, considering NADP(H) and NAD(H), closed, which underlines the consistency of the data. NADH consumption did not fully match the corresponding formation, which resulted in an apparent excess. This coincided with an apparent NADPH limitation and points at the presence of additional NADPH sources in *B. succiniciproducens* (Becker et al., 2013). Generally, the supply of NADPH was rather low, as compared to that in other microorganisms.

4.4. Evaluation of phenotypes within the feasible flux space: fructokinase is the key for efficient succinate production from sucrose

It was now interesting to benchmark the created strains and assess the impact of our findings on industrial succinate production in the genomic context. Computational modeling of the metabolic network of *B. succiniciproducens* provided the entire set of thermodynamically and

stoichiometrically feasible cellular states: several thousand elementary flux modes with different efficiency regarding succinate and biomass formation (Poblete-Castro et al., 2013). This allowed two highly important evaluations. The first one identifies the impact of the discovered fructokinase on the succinate production capacity. *B. succiniciproducens*, possessing this enzyme, can produce succinate from sucrose up to a theoretical yield as high as 3 mol mol^{-1} (Fig. 9). However, without fructokinase, the maximum yield is only 2 mol mol^{-1}. It can be concluded that fructokinase is an essential enzyme for high-level succinate production from sucrose. The second evaluation benchmarks the strains, created in this work by integrating them into the modelled flux space. The succinate yield of 2.5 mol mol^{-1}, achieved during the fed-batch process, reached 85% of the maximum yield and approached the predicted theoretical optimum. Taking into account that the upper boundary at zero growth is hardly achievable in a realistic process, the biosynthetic power of the created cell factory is remarkable. Clearly, the performance of *B. succiniciproducens* in the fed-batch process was only feasible with substantial fructokinase contribution, further highlighting the impact of this enzyme for efficient production. Furthermore, the resulting increase in the succinate yield upon strain engineering was accompanied by reduced cellular growth, likely due to a re-direction of carbon from anabolism to product formation. The beneficial effects of the introduced mutations were most pronounced for conditions of substrate limitation. One might hypothesize that the capacity of fructokinase is sufficient to handle the entire fructose phosphorylation under conditions of limited influx of sucrose during the feed phase of production. This matches with a lack of pyruvate-based lactate formation under these conditions.

5. Conclusion

The created cell factory of the rumen bacterium *B. succiniciproducens* is applicable for improved succinate production from sucrose: the achieved titer is amongst the top three values, reported for succinate production with rumen bacteria (Ahn et al., 2016). This opens attractive possibilities to extend the raw material base for this important bulk chemical. Based on sugar cane or sugar beet, the disaccharide is naturally found at high concentration and purity. Unlike starch, it is not a food stable. Moreover, waste biomass, such as bagasse, is harvested with sucrose and is used to produce heat and electricity, thereby greatly reducing the carbon footprint of production. Therefore, sucrose-based production offers attractive economics. In addition, our findings on sucrose and previous works on glucose (Becker et al., 2013) create the possibility for intercropping in industrial succinate production with *B. succiniciproducens*, because the fermentation equipment is almost identical.

Finally, our work demonstrates the huge design power of ^{13}C metabolic flux analysis in systems metabolic engineering. As shown here and in previous work (Becker et al., 2005, 2011; Buschke et al., 2013), even rather complex metabolic networks are unraveled precisely by this technology to provide a reliable knowledge base for tailored strain development, which is otherwise not accessible.

Acknowledgements

We acknowledge Michel Fritz for technical support in analytics.

Appendix A. Supporting information

Supplementary data associated with this article can be found in the online version at http://dx.doi.org/10.1016/j.ymben.2017.10.003.

References

Ahn, J.H., Jang, Y.S., Lee, S.Y., 2016. Production of succinic acid by metabolically engineered microorganisms. Curr. Opin. Biotechnol. 42, 54–66.

Arifin, Y., Archer, C., Lim, S., Quek, L.E., Sugiarto, H., Marcellin, E., Vickers, C.E., Krömer, J.O., Nielsen, L.K., 2014. *Escherichia coli* W shows fast, highly oxidative sucrose metabolism and low acetate formation. Appl. Microbiol. Biotechnol. 98, 9033–9044.

Becker, J., Klopprogge, C., Schröder, H., Wittmann, C., 2009. Metabolic engineering of the tricarboxylic acid cycle for improved lysine production by *Corynebacterium glutamicum*. Appl. Environ. Microbiol. 75, 7866–7889.

Becker, J., Klopprogge, C., Wittmann, C., 2008. Metabolic responses to pyruvate kinase deletion in lysine producing *Corynebacterium glutamicum*. Microb. Cell Fact. 7, 8.

Becker, J., Klopprogge, C., Zelder, O., Heinzle, E., Wittmann, C., 2005. Amplified expression of fructose 1,6-bisphosphatase in *Corynebacterium glutamicum* increases *in vivo* flux through the pentose phosphate pathway and lysine production on different carbon sources. Appl. Environ. Microbiol. 71, 8587–8596.

Becker, J., Lange, A., Fabarius, J., Wittmann, C., 2015. Top value platform chemicals: bio-based production of organic acids. Curr. Opin. Biotechnol. 36, 168–175.

Becker, J., Reinefeld, J., Stellmacher, R., Schäfer, R., Lange, A., Meyer, H., Lalk, M., Zelder, O., von Abendroth, G., Schröder, H., Haefner, S., Wittmann, C., 2013. Systems-wide analysis and engineering of metabolic pathway fluxes in bio-succinate producing *Basfia succiniciproducens*. Biotechnol. Bioeng. 110, 3013–3023.

Becker, J., Zelder, O., Haefner, S., Schröder, H., Wittmann, C., 2011. From zero to hero - design-based systems metabolic engineering of *Corynebacterium glutamicum* for L-lysine production. Metab. Eng. 13, 159–168.

Bunch, P.K., Mat-Jan, F., Lee, N., Clark, D.P., 1997. The *ldhA* gene encoding the fermentative lactate dehydrogenase of *Escherichia coli*. Microbiol 143, 187–195.

Buschke, N., Becker, J., Schäfer, R., Kiefer, P., Biedendieck, R., Wittmann, C., 2013. Systems metabolic engineering of xylose-utilizing *Corynebacterium glutamicum* for production of 1,5-diaminopentane. Biotechnol. J. 8, 557–570.

Buschke, N., Schröder, H., Wittmann, C., 2011. Metabolic engineering of *Corynebacterium glutamicum* for production of 1,5-diaminopentane from hemicellulose. Biotechnol. J. 6, 306–317.

Christensen, B., Thykaer, J., Nielsen, J., 2000. Metabolic characterization of high- and low-yielding strains of *Penicillium chrysogenum*. Appl. Microbiol. Biotechnol. 54, 212–217.

da Silva, J.M., Arrabaca, M.C., 2004. Contributions of soluble carbohydrates to the osmotic adjustment in the C4 grass *Setaria sphacelata*: a comparison between rapidly and slowly imposed water stress. J. Plant Physiol. 161, 551–555.

Frey, J., 1992. Construction of a broad host range shuttle vector for gene cloning and expression in Actinobacillus pleuropneumoniae and other Pasteurellaceae. Res. Microbiol. 143, 263–269.

Gourdon, P., Baucher, M.F., Lindley, N.D., Guyonvarch, A., 2000. Cloning of the malic enzyme gene from *Corynebacterium glutamicum* and role of the enzyme in lactate metabolism. Appl. Environ. Microbiol. 66, 2981–2987.

Guettler, M.V., Rumler, D., Jain, M.K., 1999. *Actinobacillus succinogenes* sp. nov., a novel succinic-acid-producing strain from the bovine rumen. Int. J. Syst. Bacteriol. 49, 207–216.

Helanto, M., Aarnikunnas, J., Palva, A., Leisola, M., Nyyssola, A., 2006. Characterization of genes involved in fructose utilization by *Lactobacillus fermentum*. Arch. Microbiol. 186, 51–59.

Jetten, M.S.M., Sinskey, A.J., 1993. Characterization of phosphoenolpyruvate carboxykinase from *Corynebacterium glutamicum*. FEMS Microbiol. Lett. 111, 183–188.

Kiefer, P., Heinzle, E., Zelder, O., Wittmann, C., 2004. Comparative metabolic flux analysis of lysine-producing *Corynebacterium glutamicum* cultured on glucose or fructose. Appl. Environ. Microbiol. 70, 229–239.

Kim, T.Y., Kim, H.U., Park, J.M., Song, H., Kim, J.S., Lee, S.Y., 2007. Genome-scale analysis of *Mannheimia succiniciproducens* metabolism. Biotechnol. Bioeng. 97, 657–671.

Kim, T.Y., Kim, H.U., Song, H., Lee, S.Y., 2009. *In silico* analysis of the effects of H_2 and CO_2 on the metabolism of a capnophilic bacterium *Mannheimia succiniciproducens*. J. Biotechnol. 144, 184–189.

Krömer, J.O., Fritz, M., Heinzle, E., Wittmann, C., 2005. *In vivo* quantification of intracellular amino acids and intermediates of the methionine pathway in *Corynebacterium glutamicum*. Anal. Biochem. 340, 171–173.

Kuhnert, P., Scholten, E., Haefner, S., Mayor, D., Frey, J., 2010a. *Basfia succiniciproducens* gen. nov., sp nov., a new member of the family Pasteurellaceae isolated from bovine rumen. Int. J. Syst. Evol. Micr. 60, 44–50.

Laine, R.A., Sweeley, C.C., 1971. Analysis of trimethylsilyl O-methyloximes of carbohydrates by combined gas-liquid chromatography-mass spectrometry. Anal. Biochem. 43, 533–538.

Lee, J.W., Choi, S., Kim, J.M., Lee, S.Y., 2010. *Mannheimia succiniciproducens* phosphotransferase system for sucrose utilization. Appl. Environ. Microbiol. 76, 1699–1703.

Lee, P.C., Lee, S.Y., Hong, S.H., Chang, H.N., 2002. Isolation and characterization of a new succinic acid-producing bacterium, *Mannheimia succiniciproducens* MBEL55E, from bovine rumen. Appl. Microbiol. Biotechnol. 58, 663–668.

Lee, S.J., Lee, D.Y., Kim, T.Y., Kim, B.H., Lee, J., Lee, S.Y., 2005. Metabolic engineering of *Escherichia coli* for enhanced production of succinic acid, based on genome comparison and in silico gene knockout simulation. Appl. Environ. Microbiol. 71, 7880–7887.

Lee, S.J., Song, H., Lee, S.Y., 2006. Genome-based metabolic engineering of *Mannheimia succiniciproducens* for succinic acid production. Appl. Environ. Microbiol. 72, 1939–1948.

Liu, Y.P., Zheng, P., Sun, Z.H., Ni, Y., Dong, J.J., Zhu, L.L., 2008. Economical succinic acid production from cane molasses by *Actinobacillus succinogenes*. Bioresour. Technol. 99, 1736–1742.

McKinlay, J.B., Shachar-Hill, Y., Zeikus, J.G., Vieille, C., 2007. Determining *Actinobacillus succinogenes* metabolic pathways and fluxes by NMR and GC-MS analyses of ^{13}C-labeled metabolic product isotopomers. Metab. Eng. 9, 177–192.

McKinlay, J.B., Vieille, C., 2008. ^{13}C-metabolic flux analysis of *Actinobacillus succinogenes* fermentative metabolism at different $NaHCO_3$ and H_2 concentrations. Metab. Eng. 10, 55–68.

McKinlay, J.B., Zeikus, J.G., Vieille, C., 2005. Insights into *Actinobacillus succinogenes* fermentative metabolism in a chemically defined growth medium. Appl. Environ. Microbiol. 71, 6651–6656.

Melzer, G., Esfandabadi, M.E., Franco-Lara, E., Wittmann, C., 2009. Flux Design: *In silico* design of cell factories based on correlation of pathway fluxes to desired properties. BMC Syst. Biol. 3, 120.

Netzer, R., Krause, M., Rittmann, D., Peters-Wendisch, P.G., Eggeling, L., Wendisch, V.F., Sahm, H., 2004. Roles of pyruvate kinase and malic enzyme in *Corynebacterium glutamicum* for growth on carbon sources requiring gluconeogenesis. Arch. Microbiol. 182, 354–363.

Poblete-Castro, I., Binger, D., Rodrigues, A., Becker, J., Martins Dos Santos, V.A., Wittmann, C., 2013. In-silico-driven metabolic engineering of *Pseudomonas putida* for enhanced production of poly-hydroxyalkanoates. Metab. Eng. 15, 113–123.

Quek, L.E., Wittmann, C., Nielsen, L.K., Krömer, J.O., 2009. OpenFLUX: efficient modelling software for ^{13}C-based metabolic flux analysis. Microb. Cell Fact. 8.

Salvachua, D., Smith, H., St John, P.C., Mohagheghi, A., Peterson, D.J., Black, B.A., Dowe, N., Beckham, G.T., 2016. Succinic acid production from lignocellulosic hydrolysate by *Basfia succiniciproducens*. Bioresour. Technol. 214, 558–566.

Scholten, E., Dägele, D., 2008. Succinic acid production by a newly isolated bacterium. Biotechnol. Lett. 30, 2143–2146.

Scholten, E., Renz, T., Thomas, J., 2009. Continuous cultivation approach for fermentative succinic acid production from crude glycerol by *Basfia succiniciproducens* DD1. Biotechnol. Lett. 31, 1947–1951.

Schröder, H., Haefner, S., Von Abendroth, G., Hollmann, R., Raddatz, A., Ernst, H., Gurski, E., 2014. Microbial succinic acid producers and purification of succinic acid. US Patent US8673598B2.

van Winden, W.A., Wittmann, C., Heinzle, E., Heijnen, J.J., 2002. Correcting mass isotopomer distributions for naturally occurring isotopes. Biotechnol. Bioeng. 80, 477–479.

Wiechert, W., Siefke, C., de Graaf, A.A., Marx, A., 1997. Bidirectional reaction steps in metabolic networks: ii. Flux estimation and statistical analysis. Biotechnol. Bioeng. 55, 118–135.

Wittmann, C., 2007. Fluxome analysis using GC-MS. Microb. Cell Fact. 6, 6.

Wittmann, C., Hans, M., Heinzle, E., 2002. *In vivo* analysis of intracellular amino acid labelings by GC/MS. Anal. Biochem. 307, 379–382.

Wittmann, C., Heinzle, E., 2001. Modeling and experimental design for metabolic flux analysis of lysine-producing Corynebacteria by mass spectrometry. Metab. Eng. 3, 173–191.

Wittmann, C., Heinzle, E., 2002. Genealogy profiling through strain improvement by using metabolic network analysis: metabolic flux genealogy of several generations of lysine-producing Corynebacteria. Appl. Environ. Microbiol. 68, 5843–5859.

Wittmann, C., Kiefer, P., Zelder, O., 2004. Metabolic fluxes in *Corynebacterium glutamicum* during lysine production with sucrose as carbon source. Appl. Environ. Microbiol. 70, 7277–7287.

Wu, L., Birch, R.G., 2007. Doubled sugar content in sugarcane plants modified to produce a sucrose isomer. Plant Biotechnol. J. 5, 109–117.